GLIA

WILEY

RESEARCH ARTICLE

Novel potent liposome agonists of triggering receptor expressed on myeloid cells 2 phenocopy antibody treatment in cells

Christophe Boudesco[1] | Annelies Nonneman[2] | Alessandro Cinti[3] |
Paola Picardi[3] | Loredana Redaelli[3] | Sofie Swijsen[4] | Julian Roewe[5] |
Peter Reinhardt[5] | Melanie Ibach[6] | Jochen Walter[6] | Jennifer M. Pocock[7] |
Yi Ren[8] | Pierre-Alexandre Driguez[9] | Gihad Dargazanli[9] | Stephanie Eyquem[1] |
Jonathan Proto[8] | Amilcar Flores-Morales[1] | Laurent Pradier[1]

[1]Rare and Neurology TA, Sanofi, Chilly-Mazarin, France

[2]Neuroscience, Janssen Research & Development, Beerse, Belgium

[3]Cell biology, Axxam SpA, Bresso, Italy

[4]In vivo, Charles River Laboratories, Beerse, Belgium

[5]Neuroscience Discovery, AbbVie Deutschland GmbH & Co. KG, Ludwigshafen, Germany

[6]Department of Neurology, University of Bonn, Bonn, Germany

[7]Department of Neuroinflammation, University College London, Queen Square Institute of Neurology, London, UK

[8]Rare and Neurology TA, Sanofi, Framingham, Massachusetts, USA

[9]Integrated Drug Discovery, Sanofi, Chilly-Mazarin, France

Correspondence
Christophe Boudesco, Amilcar Flores-Morales, and Laurent Pradier, Sanofi R&D, Rare and Neurology TA, 1 Av P Brossolette, 91385 Chilly-Mazarin Cedex, France.
Email: cboudesco@exscientia.co.uk, amilcar.flores-morales@sanofi.com, and
Email: laurent.pradier@sanofi.com

Abstract

The receptor Triggering Receptor Expressed on Myeloid cells 2 (TREM2) is associated with several neurodegenerative diseases including Alzheimer's Disease and TREM2 stimulation represents a novel therapeutic opportunity. TREM2 can be activated by antibodies targeting the stalk region, most likely through receptor dimerization. Endogenous ligands of TREM2 are suggested to be negatively charged apoptotic bodies, mimicked by phosphatidylserine incorporated in liposomes and other polyanionic molecules likely binding to TREM2 IgV fold. However, there has been much discrepancy in the literature on the nature of phospholipids (PLs) that can activate TREM2 and on the stability of the corresponding liposomes over time. We describe optimized liposomes as robust agonists selective for TREM2 over TREM1 in cellular system. The detailed structure/activity relationship studies of lipid polar heads indicate that

Abbreviations: APP, amyloid precursor protein; Aβ, amyloid peptide; CHO, Chinese hamster ovary; CNS, central nervous system; DAM, disease associated microglia; DLS, diffraction light scattering; DOPC, 1,2-dioleoyl-sn-glycero-3-phosphocholine; DOPS, 1,2-dioleoyl-sn-glycero-3-phosphoserine; DPPC, 1,2-dipalmitoyl-sn-glycero-3-phosphocholine; GalCer, galactoside cerebroside; HEK, human embryonic kidney cell line 293; iPSC-Mg, induced pluripotent stem cell derived microglia; KO, knock-out; NDD, neurodegenerative diseases; PDI, polydispersity index; PC, phosphatidyl-choline; PL, phospholipids; PLCγ2, phospholipase Cγ2; PS, phosphatidyl-serine; PMA, phorbol myristate acetate; RNP, ribonucleoprotein; SAR, structure activity relationship; SM, sphingomyelin; SN, supernatant; Syk, spleen tyrosine kinase; TREM2, triggering receptor expressed on myeloid cells 2; WT, wild type

negatively charged lipid heads are required for activity and we identified the shortest maximally active PL sidechain. Optimized liposomes are active on both TREM2 common variant and TREM2 R47H mutant. Activity and selectivity were further confirmed in different native TREM2 expressing cell types including on integrated cellular responses such as stimulation of phagocytic activity. Such tool agonists will be useful in further studies of TREM2 biology in cellular systems alongside antibodies, and in the design of small molecule synthetic TREM2 agonists.

KEYWORDS
agonist, Alzheimer's disease, liposomes, phosphoplipids, triggering receptor expressed on myeloid cells 2

1 | INTRODUCTION

Supported by an ever-growing body of literature, the Triggering Receptor Expressed on Myeloid cells 2 (TREM2) is now considered a target for next generation medicine to treat neurodegenerative diseases (NDD). TREM2 is an innate immunoglobulin superfamily cell surface receptor expressed in the brain, specifically by microglia, a specialized central nervous system (CNS) resident macrophage. Recent studies exploiting the power of high throughput single cell RNA sequencing have provided compelling evidence of TREM2's role in microglia activation and transition from a homeostatic state (Lee et al., 2018) to a disease associated (DAM) phenotype in mice and humans (Krasemann et al., 2017; Zhou et al., 2020). Several in vivo studies have confirmed the inability of TREM2 deficient microglia to acquire a complete DAM phenotype (Lee et al., 2018; Nugent et al., 2020; Parhizkar et al., 2019; Song et al., 2018), but more importantly, these studies have demonstrated the neuroprotective/neuroinflammation resolution potential of these DAMs in NDD mouse models (Parhizkar et al., 2019; Ellwanger et al., 2021; Ewers et al., 2019; Ulland et al., 2017). TREM2-activated microglia acquire critical capacities to respond, control and resolve neuroinflammation stimuli, including enhanced migration, phagocytosis, survival, proliferation and lipid/energy metabolism (Nugent et al., 2020; Ulland et al., 2017; McQuade et al., 2020; Piers et al., 2020). In parallel, human genetic studies identified that loss of function mutations in either TREM2 or its accessory protein DAP12 were causative for Nasu-Hakola disease and frontal temporal dementia (Guerreiro et al., 2013; Paloneva et al., 2002). The rare TREM2 R47H variant is a strong genetic risk factor for Alzheimer's Disease, and genome wide association studies have further linked the TREM2 gene to several NDDs (Guerreiro et al., 2013; Borroni et al., 2014; Cuyvers et al., 2014; Li et al., 2020). Collectively, the evidence of a pivotal role for TREM2 in microglial neuroprotection have established the rational to design TREM2 activation targeting therapies (Lee et al., 2018; Nugent et al., 2020; Parhizkar et al., 2019; Song et al., 2018; Keren-Shaul et al., 2017; Andreone et al., 2020). Several groups have reported the identification of TREM2 activating antibodies targeting the stalk domain and leading to TREM2 dimerization/clustering. In vivo, these antibodies have demonstrated the beneficial effects of TREM2 engagement in different APP mutant expressing Alzheimer mouse models (APP-NL-G-F, 5XFAD) (Ellwanger et al., 2021; Fassler et al., 2021; Schlepckow et al., 2020; Wang et al., 2020) with some already in clinical trials (Wang et al., 2020). In addition to clustering antibodies, it would be useful to design synthetic TREM2 agonists acting on the natural ligand site in the IgV-fold to further study TREM2 biology with alternate agonists and potentially provide early leads for new therapeutic modalities. A well characterized TREM2 ligand is $A\beta$, which has been reported to bind to TREM2 in its oligomeric but not its monomeric or fibrillar forms (Vilalta et al., 2021; Zhao et al., 2018; Joshi et al., 2021). In addition, a broad category of TREM2 ligands is represented by charged lipophilic molecules, such as anionic and zwitterionic lipids, glycolipids, lipoproteins, and apolipoproteins (notably ApoE) (Atagi et al., 2015; Cannon et al., 2012; Wang et al., 2015; Yeh et al., 2016). Phosphatidyl serine (PS) exposed on apoptotic bodies in particular has been proposed by several studies to activate TREM2 (Wang et al., 2015; Kober et al., 2016; Poliani et al., 2015; Shirotani et al., 2019; Cosker et al., 2021; Garcia-Reitboeck et al., 2018) and a cocrystal structure resolved the PS binding site on TREM2 IgV fold (Sudom et al., 2018). PS has also been considered as an "eat me" signal for microglial cells (Scott-Hewitt et al., 2020). This exciting observation could suggest that specific TREM2 signaling engagement could be achieved using a structurally defined phospholipid (PL) agonist. However, most of these studies with defined lipids have analyzed TREM2 activation in cells seeded onto lipid-coated plates and evaluating activation after several hours of incubation. As absorption of hydrophobic molecules on plastic can alter their conformation, this system has significant limitations to mirror the lipid structure of soluble apoptotic vesicles. Indeed, conflicting data have even been reported with some of these lipid structures across different studies, as exemplified by phosphatidyl choline (PC) and the non-phosphatidyl lipid sphingomyelin (SM). PC was initially described as a potent TREM2 engager (Wang et al., 2015; Poliani et al., 2015). However, Shirontani et al. have recently reported the inactivity of PC in their plate coated lipid system (Shirotani et al., 2019). On the opposite, PC and SM reconstituted liposomes were found to have the same activity as TREM2 binding lipid PS (Nugent et al., 2020), highlighting the

inconsistencies observed across studies. In addition, the stability of such lipid preparations overtime remains an issue for regular laboratory use.

Here, we describe an optimized liposome composition with long term stability that allows a reliable and detailed structure activity relationship studies of lipid polar heads as TREM2 agonists in cellular systems. Significant differences were noted with previous reports on PL head TREM2 specificity. We identified the shortest maximally active sidechain leading to an optimized robust TREM2 agonist that can be used by simple addition to cellular cultures. We demonstrate their activity on both TREM2 common variant and TREM2 R47H mutant and their specificity versus the closely related TREM1 receptor. Activity and selectivity were further confirmed in native TREM2 expressing cell line including human IPS-derived microglia, using phagocytic activity as an integrated cellular response.

2 | MATERIAL AND METHODS

2.1 | Primary, secondary antibodies and western blot

The primary antibodies were obtained from the indicated providers: goat polyclonal anti-hTREM2 (AF1828, R&D Systems), rabbit monoclonal anti-hTREM2 (ab209814), rabbit monoclonal anti-DAP12 (ab124834 Abcam), rabbit monoclonal anti-APP (CST29765), rabbit monoclonal anti-GAPDH (CST 5174), mouse monoclonal anti-β-Actin (A2228, Sigma Aldrich), goat polyclonal anti-hTREM1 (AF1278, R&D Systems), monoclonal mouse anti-TREM1 (MAB1278, R&D Systems), goat polyclonal F(ab)2 IgG (H + L) PE-conjugated Antibody (F0102B), monoclonal Mouse IgG1 anti-human TREM-1 PE-conjugated Antibody (FAB1278P), monoclonal Rat IgG2B anti- Human/Mouse TREM2 PE-conjugated Antibody (FAB17291P).

For Western blot analysis, cell pellets were lysed using RIPA Buffer (R0278 Sigma Aldrich) supplemented with Halt™ Protease and Phosphatase Inhibitor Cocktail (78,446, Thermo Fisher) for 15 min on ice. After clarification by 12 min centrifugation at 15,000 g, cell lysates protein concentration was measured using Pierce™ BCA Protein Assay Kit (23,225, Thermo Fisher). Cell lysates (10 μg/ml) were run on precast gel NuPAGE™ 4%–12%, Bis-Tris, 1.5 mm, Mini Protein Gel, 15-well (NP0336BOX, Invitrogen) in Invitrogen's Western blot device using NuPAGE™ MES SDS Running Buffer (NP0002, Invitrogen), and transferred on PVDF membrane using iBlot 2 Gel Transfer Device (Invitrogen). After 1 h blocking in TBS-0.1% Tween 20%–5% BSA solution, membranes were exposed to primary ab (1/5000 dilution) overnight at 4°C with gentle shaking. The next day, membrane were washed four times using TBST buffer and incubated with anti-isotype secondary antibodies (1/10000, sc-2005 and sc-2004) 45 min at room temperature (RT). Membranes were eventually washed another four times after secondary antibody incubation and exposed to ECL solution Pierce™ ECL Western Blotting Substrate (32,109,

Thermo Fisher). Signal was acquired in a AI600 Amersham Chemiluminescent Imager.

2.2 | Liposome preparation

Liposome preparation protocol is adapted from a previously described publication (Sudom et al., 2018). Most of the liposomes produced in the present manuscript are using the formulation 3, corresponding to a 50/32/18 molar ratio of CHO/ 1,2-Dioleoyl-sn-glycero-3-phosphocholine (DOPC)/PL respectively. Molar ratios of initial liposome formulations are detailed in corresponding figure legends. Chloroform-dissolved lipids (see list and source down below) were mixed in a V bottom glass tube containing 0.5 ml of absolute ethanol. The solvents were removed by rotary evaporation at 45°C under gradually lowered pressure exposure (from 999 mbar to 0) to obtain a thin lipid film. After brief Argon exposure, the lipid film was dried under vacuum at RT overnight. After complete drying, the film was briefly exposed to argon gas before hydration with a phosphate buffer (PBS 1X pH 7.4, no Ca & Mg, Thermo Fisher) during 30 min at 45°C under agitation to produce a multilamellar lipid solution at a total lipid concentration of 1.72–1.75 mg/ml. The flask was successively sonicated in an ultrasonic water bath during 2 mn at 25°C, and then a second time using an immersed probe tip ultrasound (Vibracell 75,115, Bioblock Scientific, 500 W, 10 s pulse with 30 s interval between pulse, six times, at 25°C and 25% power.

The resulting emulsion was then extruded by passaging 2 ml samples 11 times through a mini extruder (Avanti Polar Lipids) equipped with a polycarbonate membrane (pore size 100 nm). A first round of liposome quality control is realized by Dynamic Light Scattering to address liposome size, polydispersity index (PDI), and zeta potential (1/50 PBS dilution, Zetasizer nano series, Malvern), and liposome activity is subsequently validated in TREM2/DAP12 expressing cell lines (see below). Liposome solution was stored at 4°C until further use. Freezing to −20°C led to sharp decrease in TREM2 activation potential (data not shown).

Phospholipid were all purchased from Avanti lipids (catalog reference in bracket) followed by short name used in the paper: 1,2-dioleoyl-sn-glycero-3-phosphocholine (850375) for DOPC; 1,2-Dipalmitoyl-sn-glycero-3-phosphocholine (850355) for DPPC; 1,2-Dioleoyl-sn-glycero-3-phosphate (840875) for DOPA; 1,2-Dioleoyl-sn-glycero-3-phosphoethanol (840513) for DOPEth; 1,2-Dioleoyl-sn-Glycero-3-Phospho (Ethylene Glycol) (870302) for DOPEG; 1-stearoyl-2-oleoyl-sn-glycero-3-phospho-1′-rac-glycerol (840503) for SOPG; 1,2-Dioleoyl-sn-glycero-3-phospho-L-serine (840035) for DOPS; 1,2-distearoyl-sn-glycero-3-phosphoethanolamine (850715) for DSPE; 1,2-distearoyl-sn-glycero-3-phosphoinositol (850143) for DSPInositol; N-stearoyl-D-erythro-sphingosylphosphoryl-choline (860586) for SEPC; 3-O-sulfo-D-galactosyl-ß1-1′-N-[2″(R)-hydroxystearyl]-D-erythro-sphingosine (860842) for SulfoGalCer, D-galactosyl-ß-1,1′-N-stearoyl-D-erythro-sphingosine (860844) for GalCer, Total Cerebrosides brain (131303), oxidized 1-palmitoyl-2-arachidonoyl-sn-glycero-3-phosphocholine (870604) for oxPAPC;

1,2-dioleoyl-sn-glycero-3-phosphomethanol (840420) for DOPMeth; 1,2-dioleoyl-sn-glycero-3-phosphopropanol (860103) for DOPProp.

2.3 | TREM1/DAP12 cell line generation

Briefly, 293HEK cell were transfected using 30 μg of pcDN3-blast-DEST TREM1 (blasticidin resistance) DNA and pcDNA3-neo-DEST DAP12 (geneticin) DNA expression vector and transfected using lipofectamine 2000 reagent in a T75 flask. 2 days after transfection, stably integrating clones were selected using a 10 μg/ml final concentration for blasticidin and 1 mg/ml of geneticin. Growing clones were further amplified and checked for TREM1/DAP12 expression by western blot and flow cytometry. Functional validation of the cell line was achieved by measuring p-Syk induction signal upon AF1278 stimulation (TREM1 targeting, 10 μg/ml) and inactivity of AF1828 antibody (TREM2 targeting, 10 μg/ml).

2.4 | Cell culture

Stably expressing TREM2 WT, R47H, T66M human embryonic kidney HEK293 clonal cell lines were described previously and grown in DMEM medium supplemented with 10% heat-inactivated FCS and 1% Penicillin/Streptomycin at 37°C in a 5% CO2 atmosphere (Ibach et al., 2021), while THP1 cells were cultivated in the same condition but using an RPMI based media. The HEK293 TREM1/DAP12 cell line (clone H) was maintained in the same condition as the TREM2 expressing cell lines.

iCell IPSC derived microglia were purchased from Cellular Dynamics, using TREM2 common variant (R1131) and homozygous P59AfsTer16 and P59AfsTer46 TREM2 frameshift mutated iCell Microglia TREM2 HO (R1202) lines. Cells were handled and maintained according to manufacturer's media and instructions. Briefly, cells were thawed 24 h before the experiment and plated at 15,000 cells per well in PEI coated plates in maintenance media (four wells per conditions). 24 h after plating, cells were starved for 4 h using no FBS containing DMEM before stimulation using agonist antibody or liposome during indicated time and concentrations.

Home-grown IPSC derived microglia were generated according as described (Haenseler et al., 2017) using the following iPSC lines: BIONi010-C (isogenic control line) and BIONi010-C-17 (TREM2 KO) both obtained from EBiSC (https://cells.ebisc.org/search). Only precursors from harvest week 6 to harvest week 13 were collected to undergo differentiation into microglia by culturing them for 14 days in Advanced DMEM/F12 (ThermoFisher, #12634-010) supplemented with 1 mM Glutamax (ThermoFisher, #35050-038), 100 U/ml penicillin and 100 μg/ml streptomycin (ThermoFisher, #15140-122), 50 μM 2-mercaptoethanol (ThermoFisher, #31350-010), 100 ng/ml IL-34 (PeproTech, #200–34) and 10 ng/ml GM-CSF (ThermoFisher, #PHC2015) in uncoated μClear 96-well plates (Greiner Bio-one, #655090) at a density of 30,000 cells/well in a volume of 200 μl medium/well, or in uncoated 384-well plates (Greiner #781091) at a density of 7500 cells/well in a volume of 40 μl medium/well.

On day 14 of microglia differentiation, 150 μl of the 200 μl microglia medium was removed from the microglia. The remaining 50 μl of medium present on the cells was supplemented with 50 μl of a 2x liposome solution of respectively DOPS, DOPEG or DPPC in microglia medium. The microglia were incubated with the liposomes for 2 min at RT. As a control, some wells with microglia were treated with 20 μg/ml of the TREM2 agonistic antibody (R&D systems, #AF1828) or the IgG control antibody (R&D systems, #AB-108-C) for 5 min at RT.

2.5 | Cellular functional assay and AlphaLISA technology

Phosphoprotein detection in cell lysates after stimulation was performed by AlphaLISA technology according to manufacturer's instructions (AlphaLISA® SureFire® Ultra™, Perkin Elmer), using p-Syk 525/526 (ALSU-PSYK-10 K), SYK (ALSU-SYK-10 K), P-AKT 1/2/3 (ALSU-PAKT-B500), Total AKT (ALSU-TAKT-B500), P-PLCγ2 Y759 (ALSU-PPLCG2-B500) kits. Briefly, cells were plated 18 h in Corning® BioCoat™ Plate 96 w PDL coated at a density of 15,000 cells/w (HEK based reporter cell lines), 50,000 cells/w (THP1) and 15,000 cells/w (Cellular Dynamics IPSC-MG). Of note, THP1 were preconditioned with 35 ng/ml TGFβ1 during the 18 h plating time (130-095-066, Miltenyi Biotec) as it was found to improve TREM2 stimulation response (not shown). The next day, cells were starved for a duration of 6 h in FBS-free DMEM medium. A 96 w master plate was freshly prepared to contain activating mix in FBS-free DMEM medium and added to the target well at indicated time after removal of the starvation medium. After activation, cell supernatants were removed, and cells lysed by adding 50 μl of 1X AlphaLISA lysis buffer per well for 10 min at RT with gentle shaking. Lysates were subsequently stored at −20°C and used for phospho-protein measurement in 384 w AlphaLISA plate according to manufacturer's instruction. For experiment including Syk Inhibitor VI R406 (505,819, Merck), starvation medium was added of 5 μM of R406. Each p-protein signal is normalized according to its corresponding total protein signal. For instance, with p-Syk, the induction signal plotted is the ratio of p-Syk normalized to total Syk signal for a treatment condition compared to vehicle treated cells.

A slightly modified protocol was adapted for home-grown iPS-MG. After incubation with the liposomes or the controls, all the medium was removed from the iPSC-derived microglia. Microglia were lysed with a 2x AlphaLISA lysis buffer solution (prepared according to the manufacturer's instructions) for 10 min on a shaker (350–400 rpm) at RT, followed by the addition of an equal volume of distilled H2O to obtain a final 1x concentrated lysis buffer suitable for the AlphaLISA® SureFire® Ultra™ immunoassays (PerkinElmer).

To evaluate TREM2 downstream signaling activation the following assay were used: phosphorylated Syk, total Syk (as above) and total GAPDH (#ALSU-TGAPD-A10K). AlphaLISA assays were performed in white 384-well OptiPlates (PerkinElmer) according to the manufacturer's protocol. In brief, 10 μl of fresh cell lysate was transferred to a 384-well Optiplate followed by the addition of 5 μl of Acceptor mix. For the p-Syk AlphaLISA 10 μl of pure cell lysate was

used, whereas for the Total Syk and GAPDH AlphaLISA the pure cell lysate was further diluted 1/5 in lysis 1x buffer. After 2 h of incubation at RT 5 µl Donor mix was added in a light reduced environment, followed by incubation for 1 h protected from light. Plate reading was done using the EnVision plate reader (PerkinElmer). All samples were run in technical triplicates. For data analysis, the average of the technical triplicates was calculated per sample followed by background subtraction. p-Syk and Total Syk levels were normalized to the relative GAPDH levels and scaled relative to the microglia samples treated with 50 µg/ml DOPS.

For dose/response study in 384-well plate a slightly modified protocole was used for p-Syk and total Syk assays. AlphaLISA assays were performed in gray 384-well AlphaPlates (PerkinElmer) according to the manufacturer's protocol. In brief, 10 µl of fresh cell lysate, for both p-Syk and Total Syk levels quantification, were transferred to a 384-well AlphaPlate followed by the addition of 5 µl of Acceptor mix. After 1 h of incubation at RT, 5 µl Donor mix was added in a light reduced environment, followed by incubation for 1 h protected from light. Plate reading was done using the PHERAstar FSX plate reader (BMG LABTECH). All samples were run in technical quadruplicates. For data analysis, the average of the technical quadruplicates was calculated. p-Syk levels were normalized to the relative total Syk levels and scaled relative to the untreated microglia samples.

2.6 | Flow cytometry

All cell lines were stained using the same procedure. Briefly, 100,000 cells were transferred into Corning low binding U-bottom 96 w plate and centrifuged at 4°C 5 min 300 g. Cells were incubated 10 min on ice with FcR Blocking Reagent, human (Miltenyi Biotec). Cells were spun down and subsequently incubated with staining PE conjugated primary antibodies for 15 min on ice (1/100 diluted in 5% PBS BSA, goat polyclonal F(ab)2 IgG (H + L) PE-conjugated Antibody (F0102B), monoclonal Mouse IgG1 anti-human TREM-1 PE-conjugated Antibody (FAB1278P), monoclonal Rat IgG2B anti- Human/Mouse TREM2 PE-conjugated Antibody (FAB17291P). After incubation, cells were washed 3 times before signal acquisition using a MACSQuant Analyzer 10.

2.7 | Liposome cell internalization/fusion

For liposome internalization/fusion experiments, formulation three based liposomes were generated but using a PL fraction containing 17% of DOPS or DPPC and 1% of labeled 18:0 Cy5.5 PE (Avanti lipids 810,346). THP1 cells were plated in 96 multiwell PDL-coated plate as described for AlphaLISA experiments and treated with 25 µg/ml of DOPS or DPPC labeled liposomes, after starvation for 4 h in FBS-free media in presence or absence of 5 µM endocytosis inhibitor cytochalasin D (C8273-1MG, Merck). Fluorescent liposomes were incubated for indicated time before wash using ice cold PBS 5% BSA. PDL coated cells were detached using a 5 min 50 µl TRYPLE treatment

(Thermo Fisher), suspended in 100 µl of 5% BSA containing medium before signal acquisition using a MACSQuant Analyzer 10. The Mean of Fluorescence of cells exposed to liposomes was calculated and expressed as a ratio of liposome treated cells versus non treated cells.

2.8 | TREM2 shedding analysis by ELISA and western blot

TREM2 HEK293 cells ($0.3x10^6$ c/w) were plated in 24 w plate for 18 h in complete medium before incubation with the activating mix comprising medium alone (no FBS), 5 µM ADAM inhibitor GI254023X (3995, Merck Millipore) and GM6001 (2983, Merck Millipore), TREM2 stalk targeting antibody 4B2A3, and liposome, all diluted in FBS-free media. After 6 h incubation, supernatants (SN) were harvested and cleared of cell debris by centrifugation (10 min, 5000 g) and stored at −20°C. For ELISA sTREM2 measurement, SN (45 µl) was processed with the Human TREM-2 ELISA Kit (RAB1091-1KT, Sigma Aldrich) according to manufacturer's instructions. It was verified that 4B2A3 TREM2 targeting antibody used for cell activation was not interfering with the sTREM2 ELISA assay by running the ELISA on a reference cell supernatant spiked with progressive higher concentrations (1/5/10 and 20 µg/ml) of 4B2A3 before ELISA test (data not shown). For immuneblot, samples underwent a 10X concentration using the Pierce™ Protein concentrator PES 10 K MWCO (88,513, Themo Fisher) during 5 min 10,000 g. SN (8 µl) were run on WB as described above (see Primary, secondary antibodies, and western blot). For quantification, densitometry analysis of each western blot was carried out using Fiji-ImageJ software and ratio presented express the band intensity of immature TREM2 38 kDa band compared to untreated cells (immature band level for each condition is first normalized of its corresponding APP level).

2.9 | Generation of TREM2 KO THP-1 cell line

TREM2 loss-of-function cell lines were generated from parental THP-1 cells by CRISPR editing (Synthego; CA) with sgRNA (GTCTCCT CCCCAGAGCTGTC) targeting exon two (ENST00000373113). Clonal populations were generated from the KO cell pool by a limiting dilution method and subsequently expanded. Knock out was validated by Sanger sequencing (Genewiz; NJ). Briefly, genomic DNA was extracted and ∼ 500 bp amplicons were generated by PCR. Double strand sequencing was performed following PCR clean up and results were analyzed using the inference of CRISPR Edits (ICE) tool (https://ice.synthego.com). A clone with a KO score >95% was selected for subsequent experiments.

2.10 | Phagocytosis

THP1 TREM2 WT and KO were seeded at a density of 50,000 cells/w into 96 w flat-bottom plates without coating (92,096, TPP) for 72 h in complete RPMI media (10%FBS) and in presence of

100 ng/ml of Phorbol 12-myristate 13-acetate or PMA (P8139, Sigma Aldrich). WT and KO cells did not present differences of morphology before and after differentiation (data not shown). On the day of the experiment, differentiation medium was replaced by starvation medium during 6 h, medium added alone or including endocytosis inhibitor cytochalasin D (5 μM), AF1828 (10 μg/ml) or liposomes (50 μg/ml). For experiments using combination with Syk inhibitor, 5 μM of R406 (505,819, Merck) was added on the target well with antibody or liposome during the 6 h starvation. After starvation/activation period, the target phagocytosis particles, e.g. 60 μg/ml pHrodo™ Red _E.coli_ BioParticles™ (P35361, Invitrogen) or 1 μg/ml Beta - Amyloid, HiLyte™ Fluor 488 – labeled (AS-60479-01 Anaspec) were added and plates gently swirled by hand. Plates were immediately placed into an Incucyte S3 device (Essenbio Bioscience) for fluorescence acquisition overtime (24 h, four well replicates per conditions, four images per well). Total Red Object Integrated Intensity expressed in RCU μm^2/ image - defining the signal above the experimentally set threshold of a pixel's intensity to be considered as phagocytosis linked fluorescence - were extracted from Incucyte software analysis tool using the following parameters: Segmentation top hat, Radius 100 μm, Edges intensity −40, Threshold 1.6 μm^2 (_E.coli_) and 10.5 μm^2 (Aβ42), Minimum Area Filters 25 μm^2, Minimum mean intensity 2 RCU (_E.coli_) and 3.5 RCU (Aβ42). Statistical analysis and graph were realized using Prism software.

2.11 | Statistical analysis

Data were analyzed using GraphPad Prism 8 (La Jolla). All data were tested for normality and subsequently analyzed by multiple comparisons Student's _t_-test or Wilcoxon-Mann–Whitney (unpaired, two-tailed). A _p_-value less than .05 was considered as statistically significant. For statistical analysis, at least three independent experiments were analyzed.

3 | RESULTS

3.1 | TREM2 engaging liposomal particles optimization

To explore the TREM2 engaging capacities of different lipid heads anchored on a liposomal particle, we first sought to optimize the liposome formulation to mimic apoptotic body composition, and to maximize signal/noise ratio, homogeneity, and stability of the particles. Relying on computational lipidomic studies of neuronal plasma membranes (Ingolfsson et al., 2014), we established a set of liposomal formulations with different molar ratios of cholesterol (CHO), which is known to provide physical stability to liposomes, 1,2-dioleoyl-sn-glycero-3-phosphocholine (DOPC) and PL (Figure 1a). We tested these formulations on a previously described TREM2/DAP12 recombinant cell line, B1 (Ibach et al., 2021), using the known TREM2 engager PS DOPS as PL fraction, and 1,2-Dipalmitoyl-sn-glycero-3-phosphocholine

DPPC as the negative control. Abbreviations and nomenclature of all lipids used is provided in Material and Method section. As a positive control for cellular TREM2 engagement in our experiments, we included stimulation with a polyclonal TREM2 agonist antibody at the concentration previously determined to provide the maximal p-Syk increase and quantified the level of phosphorylation of Syk (p-Syk) normalized to the total Syk levels. Most formulations were able to increase p-Syk in the recombinant cell line after 5 min of stimulation, but important differences in activation were observed between DOPS and DPPC in the different formulations (Figure 1a). DOPS induced a p-Syk response equivalent to the agonist antibody when formulated with DOPC only (formulation 1) and its p-Syk signal induction was further potentiated by the addition of CHO in the liposome formulation (formulations 2, 3, and 4, Figure 1a). Increasing DOPS molar percentage from 18% to 50% did not further increase the p-Syk response. DPPC provided very different results. Quite unexpectedly, the DOPC-DPPC formulation 1 provided a strong p-Syk signal, equivalent to the agonist antibody at high concentration, while a gradual increase of CHO in combination with a decrease of DOPC content led to a complete lack of activity of the DPPC-containing liposomes (formulations 3 and 4, Figure 1a). It is important to underline that under non-physiological liposome compositions (low CHO), phosphatidyl-choline appears to act as an artificial TREM2 agonist, while not with liposome lipid composition mimicking neuronal membrane compositions which, however, maintained strong TREM2 activity with phosphatidylserine. The results in B1 cells were validated in a second TREM2/DAP12 cell line although maximal stimulation levels were lower than in the B1 line (Supplemental Figure S1A). Physical properties of DOPS particles, size, PDI, and zeta potential were very similar across the 4 formulations while DPPC-containing liposomes showed a larger heterogeneity of size (PDI) for formulations 2 and 4 and larger size (Supplemental Figure S1C). Of note, the size of the particles could not be reduced further with formulation 3, even when using a 50 nm membrane extrusion (Supplemental Figure S1B).

We therefore chose formulation 3 as the reference formulation for further experiments, since it 1) better mimics natural neuronal plasma membrane, 2) provides the highest p-Syk induction signal of TREM2-binding DOPS liposome, while DPPC counterpart were completely inactive, and 3) has a good particle size, homogeneity, and stability potential. Already providing maximal signal at 18% in formulation 3, we decreased the percentage of PL (complementing formulation with DPPC) to address whether it would influence the agonist capacities. TREM2 stimulation progressively decreased at 10% and 5% and was abolished at 1% active PL (Supplemental Figure S1D). Kinetic analysis of the different TREM2 agonist types indicated that the maximum p-Syk activation was obtained at 30 min for the TREM2 antibody, whereas DOPS liposomes demonstrated a faster activation kinetic, with a maximum signal obtained at 2 and 5 min of stimulation before fading away (Figure 1b). Of note, in our reporter cells, the maximum activation obtained upon stimulation with the antibody at 30 min was equivalent to stimulation with the highest dose of DOPS liposome at 5 min (Figure 1b). We also characterized the stability of liposome preparations over time, demonstrating that the formulation
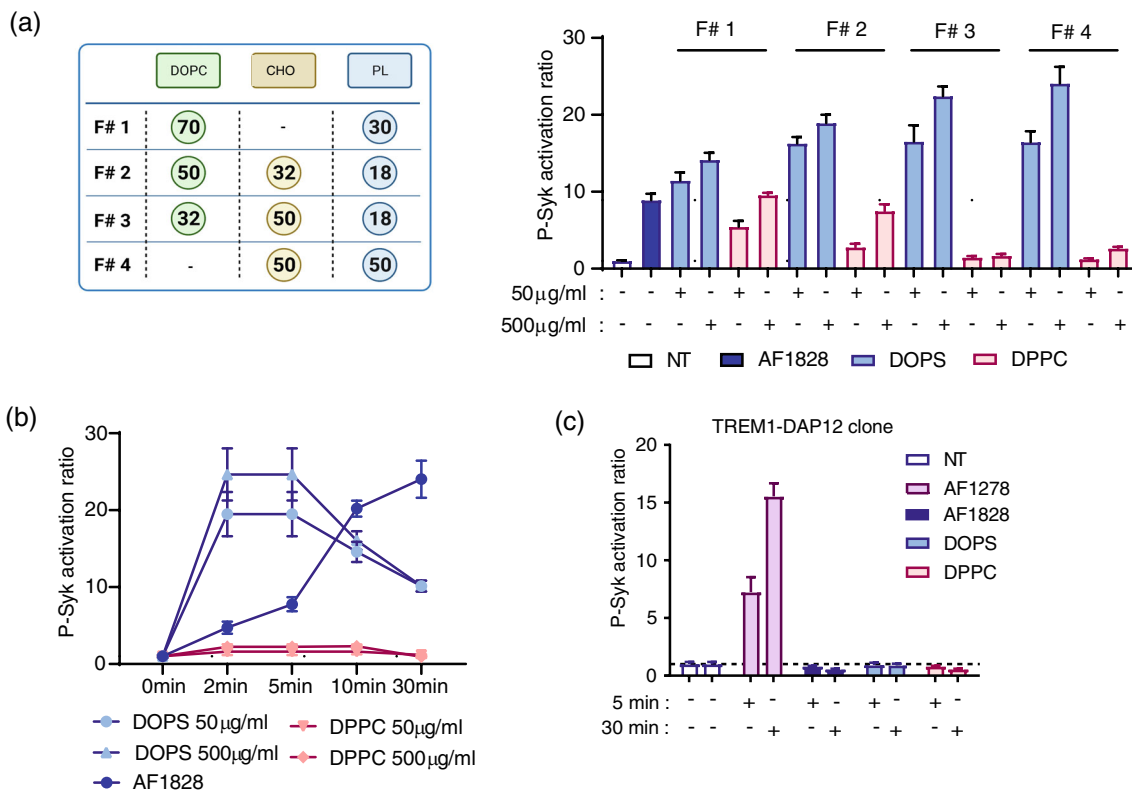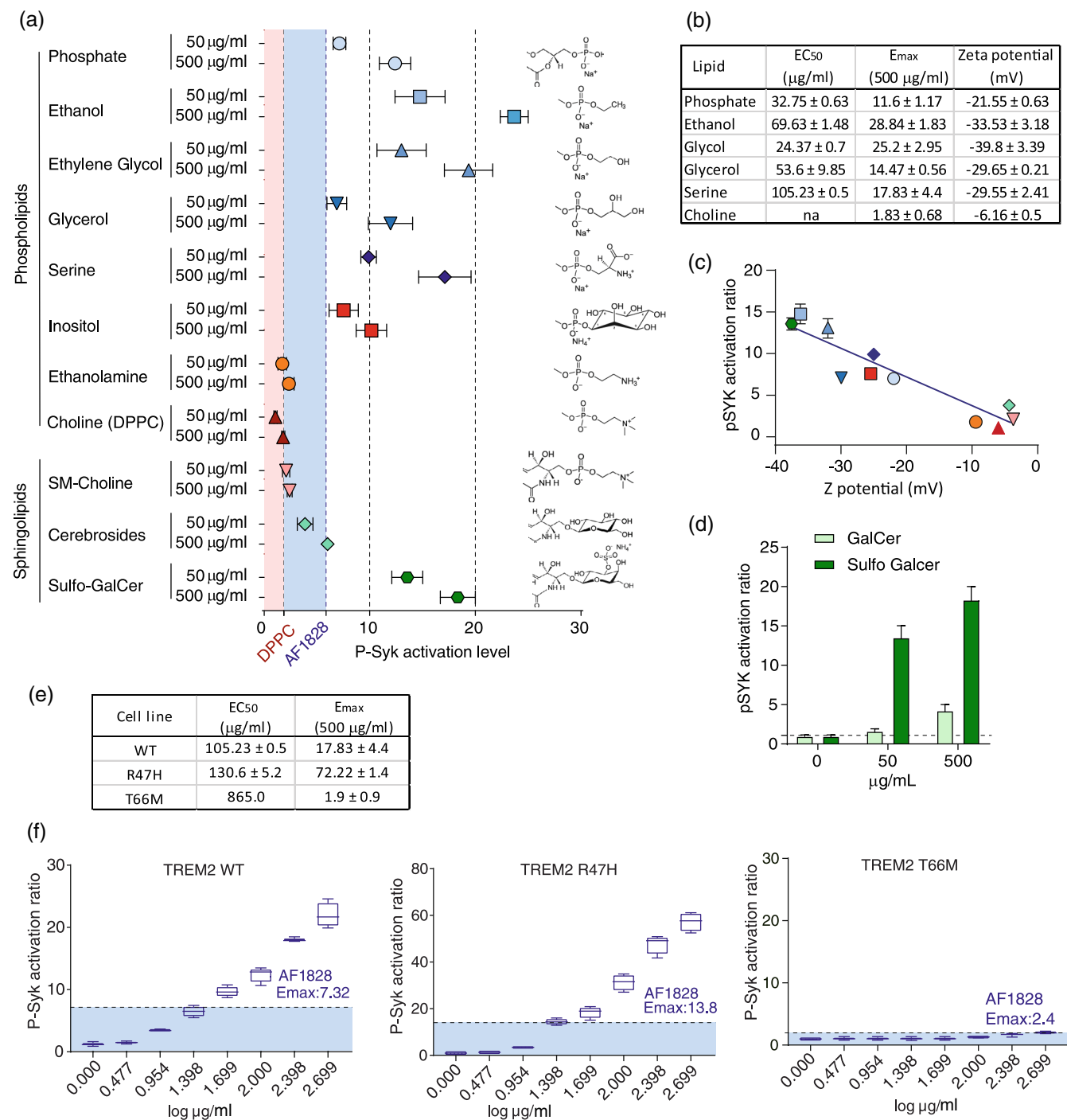
FIGURE 1 Optimized liposome particles are strong triggering receptor expressed on myeloid cells 2 (TREM2) agonists. (a) phosphorylated-spleen tyrosine kinase (p-Syk) signal increase in TREM2-DAP12 expressing human embryonic kidney (HEK) cell line (clone B1) upon antibody or liposome treatment. Starved B1 were stimulated for 5 min using AF1828 agonistic TREM2 antibody or indicated liposome formulations (F#1 to F#4 with percentage molar composition listed in left schema) at two concentrations (50 or 500 μg/ml). p-Syk and total Syk levels were quantified in lysates using AlphaLISA kits. Each p-Syk signal is normalized according to its corresponding total Syk signal. The induction signal plotted is the ratio of normalized p-Syk signal for a treatment condition compared to vehicle treated cells. Data are presented as mean ± SD from four well/condition and were representative of three independent experiments. The same data format is used for panels B and C. (b) Kinetic of p-Syk signal in AF1828 or liposome (formulation 3) treated B1 cells. Same protocol was used as in panel A but using an extended time course. (c) p-Syk signal induction in TREM1-Dap12 expressing HEK cell line (clone H). Cells were treated for 5 and 30 min using AF1278 TREM1 agonist antibody (10 μg/ml), AF1828 TREM2 antibody, or a concentration of 500 μg/ml of indicated liposome. CHO, cholesterol; DOPC, dioleoyl-phosphocholine; DOPEG, dioleoyl-phospho-(ethylene glycol); DOPS, dioleoyl-phospho-L-serine; DPPC, dipalmitoyl-phosphocholine.

3 DOPS activity was stable at 4°C for at least 3 months, while maintaining DPPC liposomes inactivity (Supplemental Figure S1E). Additionally, we tested the activity of our DOPS particles towards the TREM2-related TREM1 receptor using a TREM1/DAP12 reporter cell line (clone H). A positive control TREM1 antibody generated a time-dependent p-Syk response in clone H with a maximum signal obtained at 30 min, whereas neither the TREM2 antibody nor an agonist liposome (DOPS) was capable to induce Syk phosphorylation (Figure 1c). Collectively, these data demonstrated that our established liposome formulation 3 induced a specific TREM2 dependent p-Syk signal using an established TREM2 binding lipid, and with comparable potency to the agonist antibody.

3.2 | Structure activity studies of different lipid heads on TREM2 pathway activation

Liposomal formulation 3 was used to explore the potential of a series of PL and sphingolipid polar heads to activate TREM2 (p-Syk) in the TREM2/DAP12 reporter cell line, after 5 min of stimulation. All negatively charged PLs showed p-Syk induction capacities dose-dependently, but with variable efficacy (Figure 2a). The neutral DPPC, and its structurally related sphingolipid SM-Choline did not increase p-Syk levels, suggesting that these lipid heads are not able to engage the TREM2 receptor on these cells. Similarly, the terminal amine phosphatidylethanolamine did not show any TREM2 pathway activation. The lack of activity of DPPC was further confirmed during full concentration/response studies where DPPC showed no activity, whereas negatively charged PLs had EC_{50}'s in the μg/ml range (Figure 2b, supplemental Figure S2F). Phosphatidyl-ethanol had the highest efficacy (E_{max}) of p-Syk activation, while phosphatidyl ethylene glycol, DOPEG, had the best potency ($EC_{50} = 24,37 \pm 0.7$ μg/ml) and high efficacy, superior to the reference lipid DOPS (Figure 2b). The TREM2 activating capacities of all liposomes were further studied using the second TREM2/DAP12 expressing cell line showing similar results although producing a lower p-Syk maximal response (Supplemental Figure S2). We also verified that the key TREM2 agonist liposomes were unable to induce p-Syk in the TREM1/DAP12 cell line (Supplemental Figure S2B).

FIGURE 2 Structure activity relationship of lipid polar heads as triggering receptor expressed on myeloid cells 2 (TREM2) agonists. (a) Formulation 3 optimized liposomes with the indicated active phospholipids or sphingolipids were tested in B1 cells (5 min) at indicated concentrations, and phosphorylated-spleen tyrosine kinase (p-Syk) activation was assessed as described in Figure 1a. Data are presented as mean ± SD from four well/condition and were representative of three independent experiments. Pink shaded area corresponds to vehicle treatment range (from 0 to NT mean ± SD) while the blue dotted line right to the blue shaded space corresponds to AF1828 p-Syk induction value (mean ± SD). Molecular structures of the phospholipids polar heads are indicated. (b) Complete concentration-response analysis of key activating phospho-liposomes. EC_{50} values and maximal activating values at 500 μg/ml are reported. Nine concentration experiments were used (four wells per condition). (c) Correlation between p-Syk induction ratio and particles zeta (solvation) potential of various liposomes (color code as in panel A). Liposomal concentration was 50 μg/ml which is in the linear range of the concentration-response curve for each lipid. (d) Structural variation of gal-ceramide lipid (sulfated or not) were used to activate B1 cells for 5 min at indicated concentrations. (e–f) dioleoyl-phosphocholine concentration response curves in TREM2 wild type (WT), R47H, and T66M cell lines. (e) EC_{50} values and E_{max} are reported and were calculated from three different experiments and indicated as mean ± SD. (f) Bar graph representation of data. Note the change in Y scale for TREM2R47H, middle panel.

We next probed what could be driving the TREM2 activating capacities of the different lipids. PL head structures are shown in Figure 2a right, ordered by terminal group length. The most salient feature was that all TREM2 agonists PL carried a net negative charge including both glyco- and sphingo-lipids, while there was no direct correlation with lipid head length. While the negative charge is prominently represented by phosphate groups in the present lipid set, it could also be substituted by sulfate as in the potent sphingolipid Sulfo-GalCer compared to very low activity of uncharged cerebrosides (Figure 2a,d).

Furthermore, as TREM2 was previously described as a binder of anionic molecules and lipids, we attempted to correlate agonist activity to the zeta potential of each particle as recorded by Zetasizer/DLS, which corresponds to the liposome overall charge. There was a strong correlation ($R^2 = 0.82$) between the negative particle solvation potential and their capacity to activate TREM2 pathway (Figure 2c). To further confirm this hypothesis, we used a dual strategy consisting of testing liposome formulations bearing 1) lipid derivatives from the same structure but leading to particles of different zeta potential, and 2) lipid derivatives with structural differences but similar zeta potential. To tackle the first point, Galacto-Cerebroside (GalCer), which is uncharged (z-potential −5.23 mV) and sulfonated GalCer (z-potential -35 mV) containing liposomes were tested and only the sulfonated version of this lipid head had a clear capacity to activate a p-Syk response (Figure 2d). Second, we generated liposomes decorated with lipid head bearing phosphatidyl-alcohol derivatives with gradually extended alkyl group from phosphatidic acid to methanol, ethanol and propanol, all last three have similar zeta potential (−33.5 mV for ethanol, Figure 2b and data not shown). The three different alcohol chain length liposomes activated TREM2 similarly, with a stronger p-Syk signal compared to the corresponding phosphatidic acid liposome (Supplemental Figure S2B), which has a slightly less negative solvation potential (−21.5 mV). Therefore, the short alcohol chain phosphatidyl PL represented the most effective TREM2 agonist.

As TREM2 mutations have been reported to affect TREM2 lipid binding capacities (Wang et al., 2015; Sudom et al., 2018), the different liposomal particles were tested in TREM2 R47H/DAP12 and TREM2 T66M/DAP12 expressing cell lines (Figure 2e,f and supplemental Figure S2A). DOPS liposomes were able to engage TREM2 activation in R47H cells with similar potency as in WT-TREM2 ($EC_{50} = 130.6 ± 5.2$ vs. $105,23 ± 0.5$ for R47H vs. WT respectively), but were not able to induce p-Syk signal in the T66M mutant line (Figure 2f). In the R47H line, a higher magnitude of p-Syk signal was induced consistently by both the TREM2 polyclonal antibody and liposome agonists (Figure 2f, note difference in scale for the middle TREM2 R47H panel). TREM2 and DAP12 protein level analysis in these cell lines revealed increased DAP12 levels in the R47H versus WT expressing cells that might explain the higher p-Syk response observed in the R47H cell line while cell surface TREM2 protein expression was comparable (supplemental Figure S2D). Nevertheless, all the agonist liposomes with different lipid heads were able to activate R47H mutant quite similarly to the common variant (supplemental Figure S2A, middle panel). As expected, little activation was

obtained for TREM2 agonist antibody or the tested liposomes in the TREM2 T66M cell line (supplemental Figure S2A, right panel), which displays very low cell membrane TREM2 expression. The residual p-Syk signal observed in the T66M mutant could be accounted for by the over-expression system and leakage of a very low fraction of the mutated receptor to the cell surface, as shown by flow cytometry analysis (supplemental Figure S2D, right panel).

It was recently reported that oxidized forms of PC are enriched in Multiple Sclerosis lesions and can be cleared by microglia to limit neurodegeneration (Dong et al., 2021). We wondered if, on the contrary to normal DPPC liposome, oxidized forms of choline lipid could activate TREM2 once vectorized on a liposome entity. Using the commercially available OxPAPC from Avanti Polar Lipids, we observed that oxidized PC based liposome could induce a p-Syk signal activation even stronger than the TREM2 activating antibody (E_{max} of 9.16) whereas a DPPC liposome produced at the same time for this experiment had no activity (Supplementary Figure S2E).

It must be noted that liposome activation was maximal in medium lacking FBS. As highlighted in prior work, a protein corona is generated around zwitterionic and negatively charged liposomes in protein containing solution (Montizaan et al., 2020). We found that testing the different lipid liposomes in increasing FBS concentration media led to severe loss of activity, with variable magnitude depending on the lipid head (Supplementary Figure S2G). DOPA and DOPS demonstrated a complete loss of p-Syk induction activity with low concentration of FBS (0.5%) while DOPEG and DOPEth were less sensitive to that FBS concentration but completely inhibited at 5%.

In conclusion, we identified the minimal PL head leading to maximal TREM2 agonist efficacy, with preserved capacities on the R47H TREM2 mutant and preserved specificity over TREM1 receptor activation.

3.3 | Liposomal particles reduce TREM2 shedding in TREM2/DAP12 cell line

It has been reported that TREM2 engagement by agonistic antibodies targeting the stalk region of the receptor leads to reduced ADAM10/17-dependent shedding of the receptor, and lowered sTREM2 levels in cell culture supernatant (Ellwanger et al., 2021; Schlepckow et al., 2020). Little is known about the impact of other types of agonists on TREM2 shedding, and we wondered if liposomes could influence TREM2 shedding. After extensively washing cells to remove pre-existing sTREM2 from media, we stimulated during 6 h TREM2/DAP12 reporter cell line with a reference TREM2 monoclonal antibody agonist targeting the stalk region (Ibach et al., 2021), the agonist DOPS and DOPEG, or the signaling inactive DPPC liposomes. Secreted APP, another ADAM10/17 product was also measured as control. Secreted protein levels were quantified by ELISA assay (Figure 3a) or immunoblot (Figure 3b,c). Agonist liposomes strongly reduced sTREM2 levels in conditioned media as measured both by ELISA and by immunoblots while DPPC did not affect sTREM2 levels. The monoclonal antibody partially lowered sTREM2 levels, and this

(a)

(b)

(c)
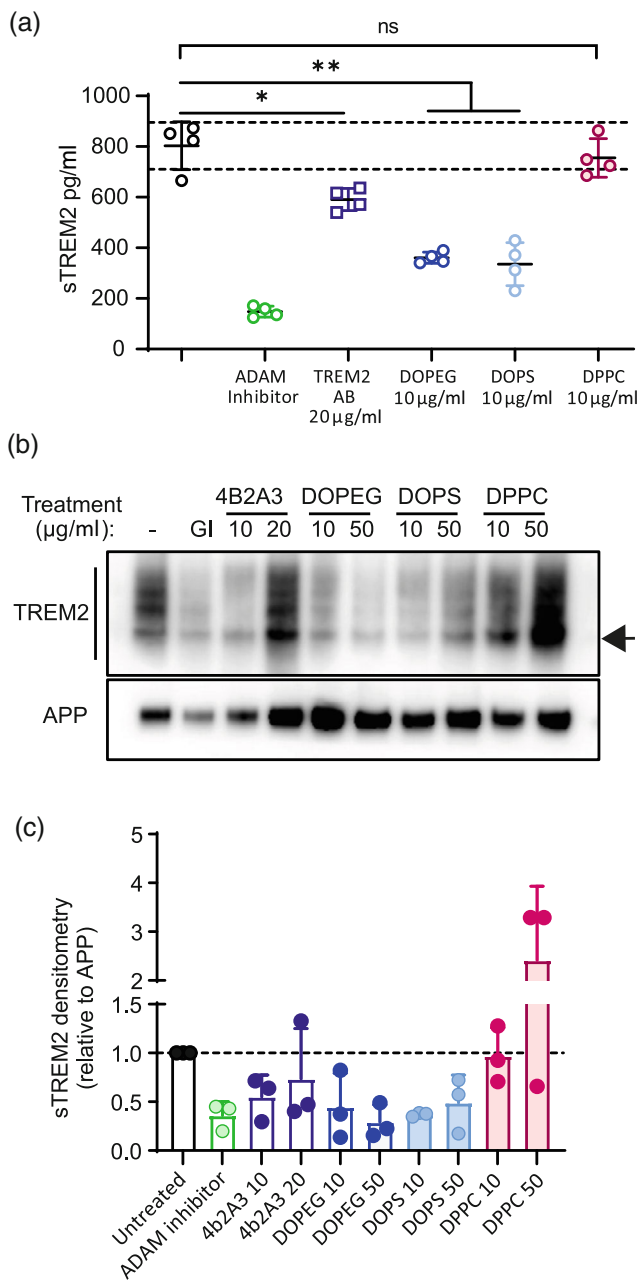
FIGURE 3 Agonist liposomes trigger triggering receptor expressed on myeloid cells 2 (TREM2) shedding similarly to stalk region targeting antibody. (a) sTREM2 level quantification in supernatant (SN) of TREM2/DAP12 expressing cell line incubated 6 h with vehicle, ADAM inhibitor, stalk TREM2 targeting antibody, or liposomes. SN were cleared from cellular debris by centrifugation (10 min, 5000xg), and sTREM2 level was measured by human TREM-2 ELISA kit (sigma Aldrich). (b) SN prepared as described in (a)- were concentrated 10 times using protein concentrator PES 10 K MWCO during 5 min 10,000xg. Concentrated SN were run on western blot to analyze TREM2 and APP level (left panel), and black arrow indicates the non-fully glycosylated form of TREM2 protein (38kD). (c) The experiment presented in (b) was reproduced three times and quantification of these experiments are presented.

was not due to 4B2A3 interference with the ELISA measurement (data not shown). As expected, the ADAM10/17 inhibitor drastically reduced TREM2 shedding. In comparison secreted APP levels were

not affected by active liposome treatments indicating that the α-secretase activity itself was not compromised.

3.4 | Liposomes activate TREM2 pathway on endogenous TREM2 expressing cell lines

We next sought to verify if the newly identified liposomal formulation and TREM2 activating lipid heads could activate the TREM2 pathway in THP1 cells, a human cell line expressing TREM2 and DAP12 endogenously. To address TREM2 dependent and independent effects, we first generated a THP1 TREM2-KO cell line by a RNP transfection system and validated the knockout by sequencing (data not shown) and at protein level by immuno-blot (Figure 4a). An 18 h TGF-β1 preconditioning was found to increase p-Syk signal induction in THP1, while p-Syk stimulation effect was also observed in the non-preconditioned cells but to a lower level (not shown). Preconditioned THP1 cells demonstrated a strong p-Syk activation by the TREM2 agonist antibody at 5 and 10 min, fading away at 30 min, while there was no response in the TREM2-KO line (Figure 4b). We verified that this was not due to a p-Syk overall signaling impairment in TREM2-KO lines by exposing both lines to the lectin concanavalin A, which is known to crosslink several cell receptors activating Syk phosphorylation independent of TREM2 (Ellwanger et al., 2021). Both TREM2 WT and KO THP1 cells responded similarly to the lectin stimulation (Figure 4b).

Next, we examined the p-Syk activation level in TREM2 WT and KO THP1 cells after stimulation with our TREM2 liposomal agonists (DOPEG, DOPS, and DOPEth) and the inactive DPPC. Similar to the TREM2 antibody stimulation, DOPEG, DOPS, and DOPEth induced a p-Syk response in WT THP1, but not in the KO THP1 (Figure 4c). The activation kinetic was faster for liposomes (E_{max} at 2 min) than for the TREM2 antibody, similarly to what was observed in TREM2 overexpressing cell lines (Figure 1b). DPPC liposomes were inactive. We confirmed these findings using a different readout, pPLCγ2, a protein downstream of p-Syk in the TREM2 signaling cascade. The results obtained were very similar to p-Syk in terms of kinetics (despite a lower activation ratio than for p-Syk signaling, Supplemental Figure S3A).

As phosphorylation of AKT (pAKT) is also a well characterized event downstream of TREM2-p-Syk signaling, we further evaluated whether both the antibody and liposomes could increase pAKT (Figure 4d). The pAKT response upon antibody stimulation was barely detectable, with a slight increase detectable upon longer stimulation (30 min). In contrast, TREM2 activating liposomes induced a stronger pAKT response, detectable from 5 min onwards, and gradually increasing up to 30 min of incubation (Figure 4d). This response was initially thought to be linked to the liposome TREM2 binding capacities, as DPPC was inactive in WT cells. However, TREM2-KO THP1 also presented a DOPEG- or DOPS-induced pAKT signal that was observed only after extended incubation times (30 min), while the antibody and DPPC did not elicit any pAKT response (Figure 4d). To further characterize the pAKT response, we stimulated the WT THP1 in the presence or absence of the Syk kinase inhibitor R406. As
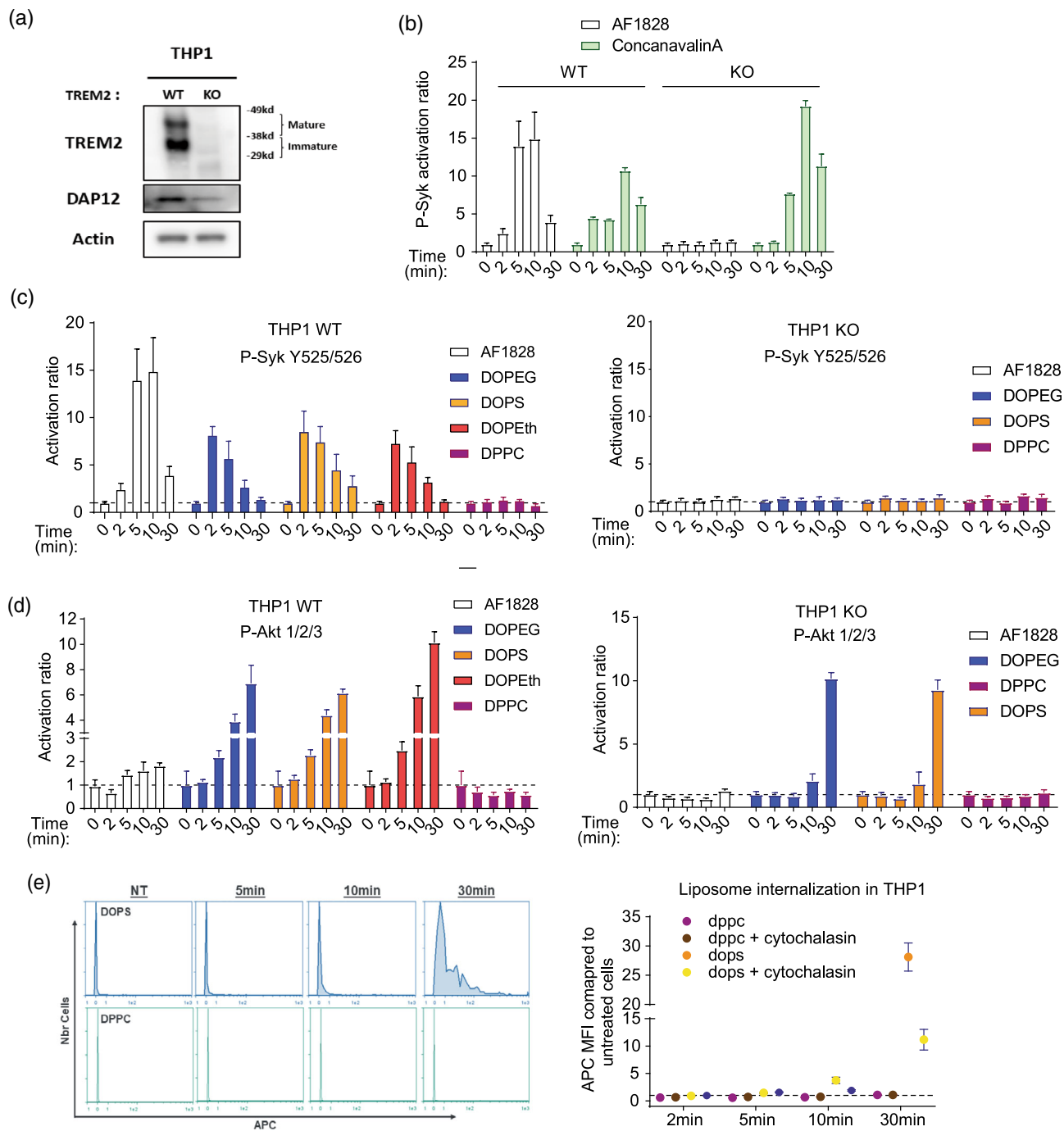
FIGURE 4 Optimized liposomes triggering receptor expressed on myeloid cells 2 (TREM2) pathway activation in natively expressing TREM2 THP1 cells. (a) TREM2 and DAP12 protein expression analysis by western blot in wild type (WT) and TREM2-KO THP1. (b) phosphorylated-spleen tyrosine kinase (p-Syk) signal induction in WT and KO THP1 stimulated for indicated time with TREM2 agonist antibody (10 μg/ml) or Concanavalin A (300 μg/ml). Briefly, 6 h starved and TGF-β1 preconditioned THP1 cells were treated with ligands for different times and p-Syk was quantified as previously described. Data are presented as mean ± _SD_ for four well/condition and were representative of three independent experiments. The same data presentation format is used for panel C and D. (c) p-Syk signaling in WT and TREM2-KO THP1 activated by TREM2 stimulating antibody or liposomal particles. Starved and TGF-β1 preconditioned THP1 were stimulated using TREM2 antibody (10 μg/ml) or liposomes formulation 3 (50 μg/ml) during indicated times. Phospho-protein signal was quantified as described previously using AlphaLISA kits. (d) similarly, pAKT signaling was analyzed in the same WT and TREM2-KO THP1 lysates generated in (c) by AlphaLISA. (e) THP1 FACS acquisition studies upon incubation with a fluorescently labeled dioleoyl-phosphocholine (DOPS) and dipalmitoyl-phosphocholine (DPPC) liposomes. Briefly, WT THP1 were plated 24 h in PDL coated plates before incubation with liposomes containing 1% of fluorescent lipid (Phosphatidyl ethanolamine Cy5.5) in presence or absence of cytochalasin D pre-treatment (5 μM). Cells were treated during indicated times and at endpoint, washed three times using 3% containing ice cold PBS, detached by pipetting flush, and analyzed by flow cytometry. Left panel staining represents an example whereas the right panel present the MFI obtained from three independent experiments (mean ± _SD_).
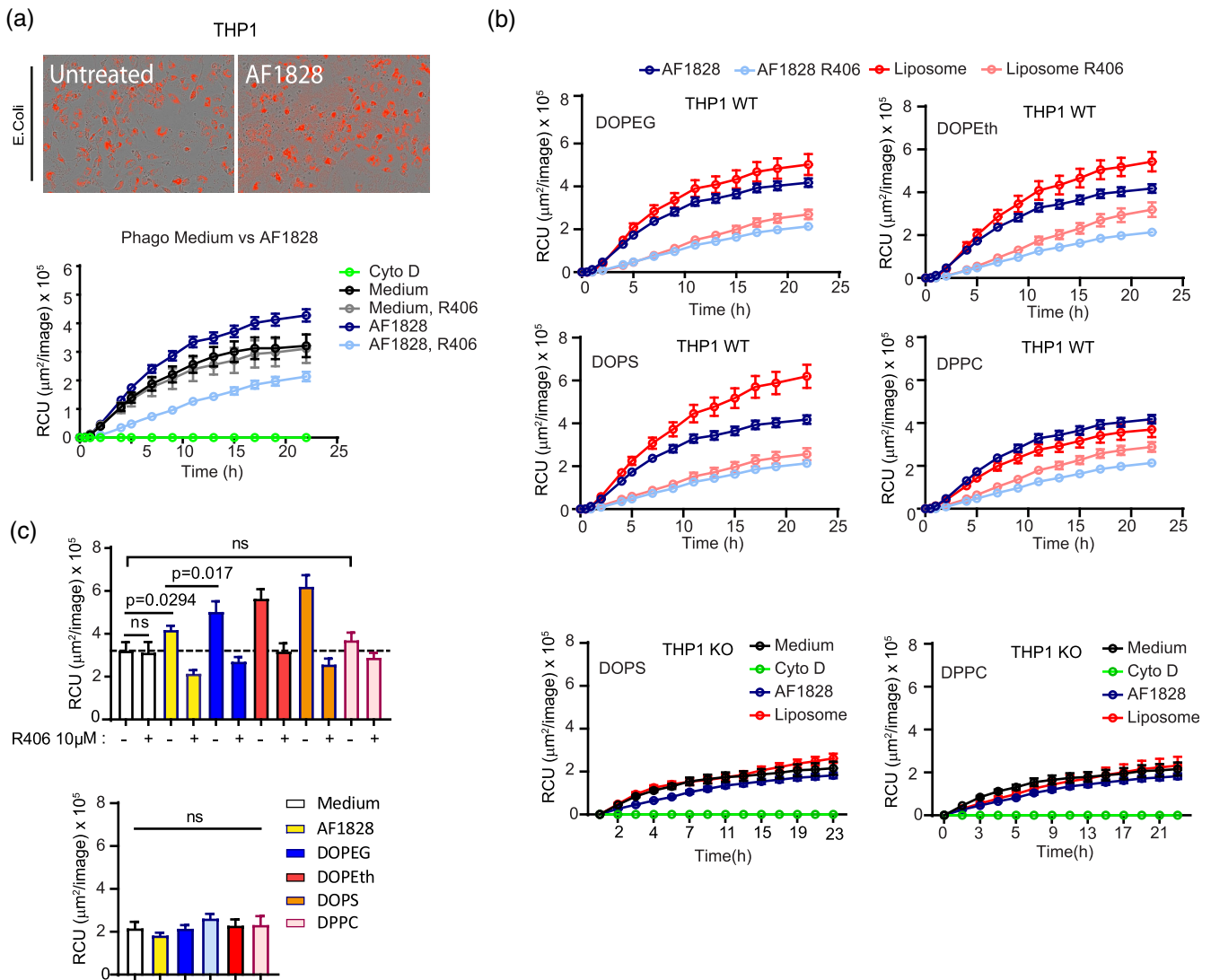
FIGURE 5   Triggering receptor expressed on myeloid cells 2 (TREM2)-activating liposomes enhance TREM2-mediated *E. coli* phagocytosis in THP1 cells. (a) Phagocytosis assay of pHrodo-labeled *E.coli* in TREM2 antibody or liposome pre-conditioned THP1. Briefly, 72 h PMA differentiated THP1 were pre-incubated 6 h with vehicle, AF1828 (10 μg/ml), liposomes (50 μg/ml), cytochalasin D (5 μM), or spleen tyrosine kinase (Syk) inhibitor R406 (5 μM). Then, 60 μg/ml of pHrodo-labeled *E.coli* was added to cells and cell fluorescence was acquired over time using Incucyte S3 (four well replicates per condition, four images per well). Specific cell fluorescence (from phagocytosed pHrodo) was calculated using Incucyte analysis software and plotted for TREM2 antibody stimulating effect over culture medium condition (mean ± *SEM*) and are representative for three experiments. In top panel are representative images at end point. (b) Test of different liposomes on *E.coli* phagocytosis activity in THP1 and Trem2-KO THP1 cells. Liposomes with different phospholipids (indicated in graphs) were tested in presence or not of Syk inhibitor R406 (5 μM) and compared to AF1828. In THP1-KO cells, only dioleoyl-phosphocholine (DOPS) and dipalmitoyl-phosphocholine (DPPC) liposomes were tested in comparison to AF1828. (c) Graph corresponding to *E.coli* phagocytosis activity of WT THP1 cells upon AF1828 and indicated liposome treatments. TREM2 KO THP1 were used according to the same procedure without R406 treatment. Phagocytosis endpoint analysis for each presented condition in WT, upper panel, and KO THP1, lower panel. Multiple *t* test was used as statistical comparison method.

expected, the rapid p-Syk activation kinetic induced by DOPEG and DOPS in THP1 cells was completely blocked by R406 (Supplemental Figure S3B, left panel). Surprisingly, while R406 blocked the pAKT signal induced at 10 min, R406 only partially lowered that response at 30 min (Supplemental Figure S3B, right panel), suggesting that the liposomal induced pAKT response was not entirely TREM2- nor p-Syk-dependent at longer time points. A recent study highlighted that negatively charged liposomes could enter/fuse into cells in a rapid

manner without involving a specific receptor facilitated endocytosis (Montizaan et al., 2020). Since the pAKT signal observed in WT THP1 cells treated with R406 was mainly observed at 30 min of stimulation, we speculated that it might be due to liposome fusion to the target cells. To this end, we designed fluorescent liposomes containing 1% of PE-Cy5.5 conjugated Phosphatidyl-Ethanolamine. We then incubated WT THP1 cells in the presence of fluorescent labeled DOPS and DPPC liposomes and monitored the cell fluorescence acquisition
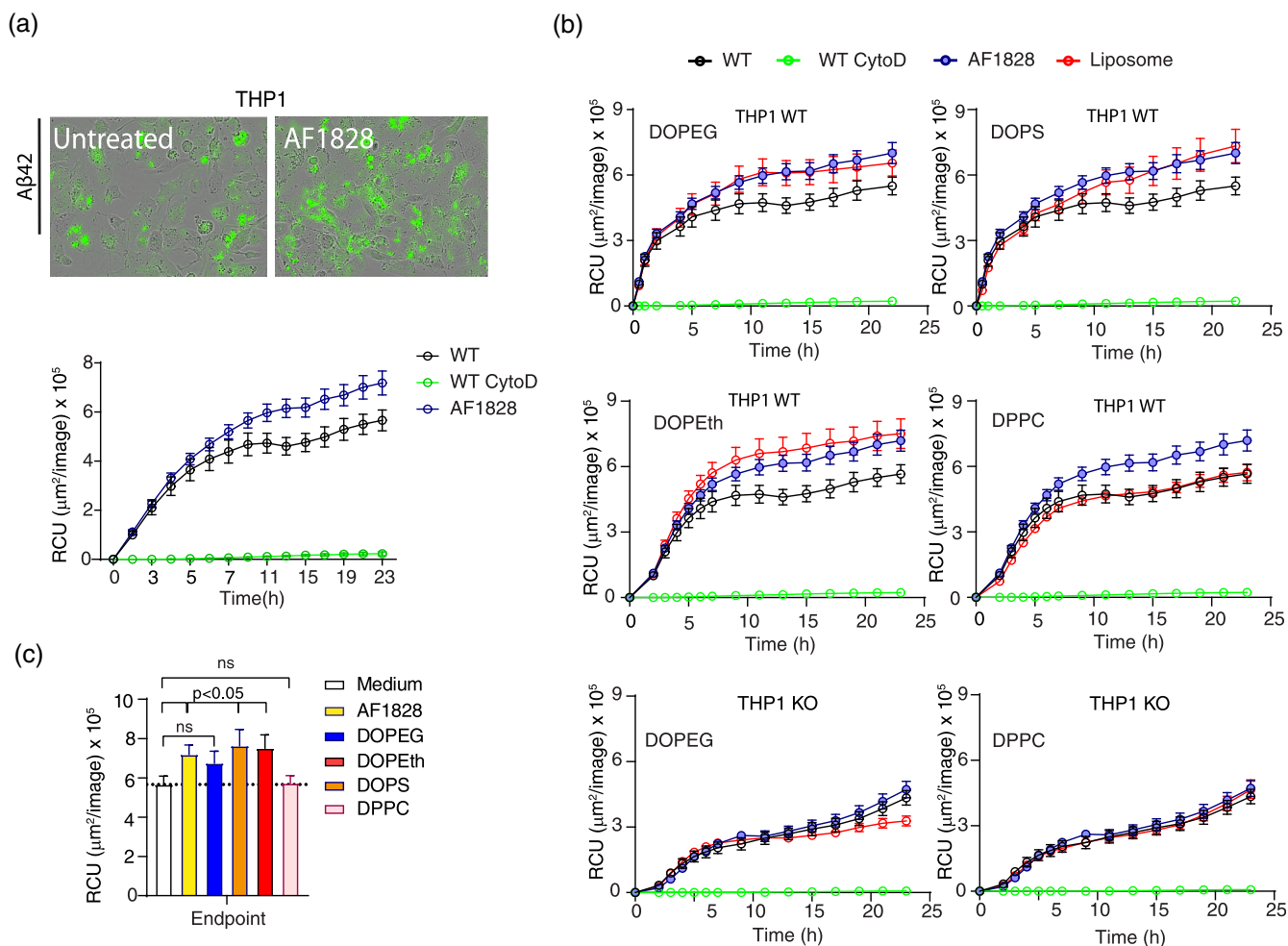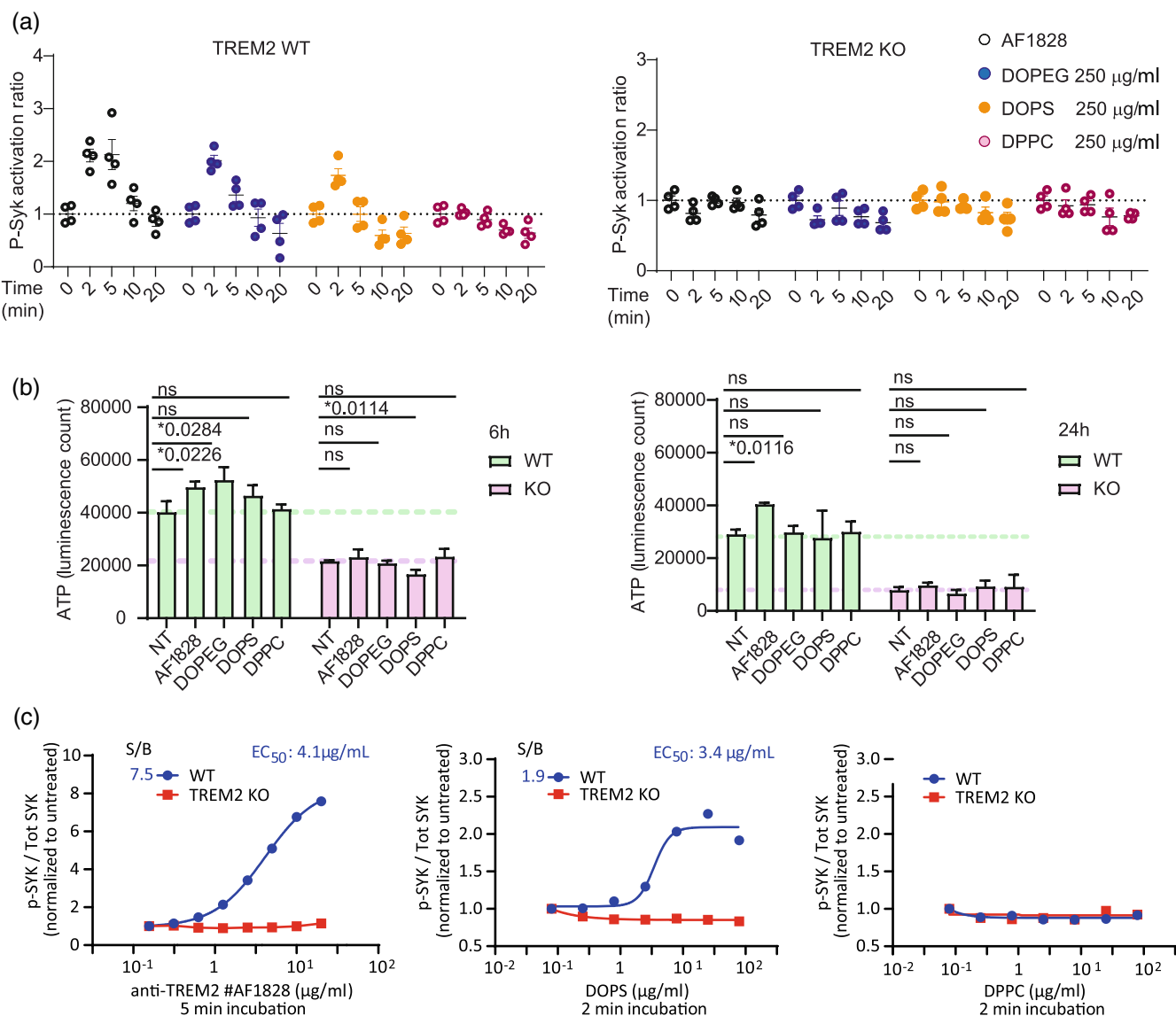
FIGURE 6 Triggering receptor expressed on myeloid cells 2 (TREM2)-activating liposomes enhance TREM2-mediated Aβ42 phagocytosis in THP1 cells. Phagocytosis assay of Aβ42 in vehicle or TREM2 antibody pre-conditionnedted THP1- similarly as described in Figure 5. Aβ42 Hilyte 488-labeled (Anaspec, 1 μg/ml) was used as substrate. (a) Representative images at end point are presented. (b) Test of different liposomes on Aβ42 phagocytosis activity in THP1 and Trem2-KO THP1 cells. Liposomes with different phospholipids (indicated in graphs) were tested and compared to AF1828. In THP1-KO cells, only DOPS and DPPC liposomes were tested in comparison to AF1828. (c) Phagocytosis endpoint analysis for each presented condition in WT THP1 using multiple *t* test.

over time by flow cytometry (Figure 4e). We observed that the DOPS liposomes induced a faint fluorescent signal in our target cells at 10 min that was clearly increased after 30 min, whereas the DPPC liposome could not lead to any fluorescent signal at the studied time points (left panel). As previously observed (Montizaan et al., 2020), DOPS liposome fusion was only partially inhibited by the endocytosis inhibitor cytochalasin D (Figure 4e, right panel) or chlorpromazine (data not shown). This important finding suggests that the pAKT signal observed at 30 min of time in WT and in TREM2-KO cells are likely due to liposome fusion to the target cells and is not TREM2-related. However, the DOPS liposome induced p-Syk and pPLCγ2 activation signals, which are observed at shorter time points, were directly related to cell surface TREM2 engagement and not to liposome fusion. Collectively, these data validate the TREM2 stimulatory effect of the DOPEG, DOPS, DOPEth liposomes in an in vitro cell model natively expressing TREM2 at physiological levels with the additional delayed activation of the Akt pathway in a non-TREM2/Syk dependent pathway.

3.5 | Liposomal particles enhance TREM2 mediated phagocytosis in THP1 cells

Next, we wanted to address if our liposomal agonist could enhance TREM2 driven integrated cellular functions. For example, TREM2 is a critical player of phagocytosis, both in a direct manner as receptor for phagocytosed substrates (Lee et al., 2018; McQuade et al., 2020; Takahashi et al., 2005) or indirectly via transcriptional effects or interaction with other receptors (Griciuc et al., 2019; Kim et al., 2017). We took advantage of the THP1 capacities to differentiate into macrophage-like cells with PMA treatment (which does not alter TREM2 level, data not shown) to question whether our liposomes could enhance the phagocytosis of different particles in culture. To this end, 72 h PMA differentiated THP1 were exposed for 6 h to TREM2 agonists (agonist antibody, TREM2 activating liposomes), non-activating liposome (DPPC), in the presence or absence of the endocytosis inhibitor Cytochalasin D, or the Syk inhibitor R406. After this

FIGURE 7 Triggering receptor expressed on myeloid cells 2 (TREM2)-activating liposomes in human induced pluripotent Stem cell derived microglia (iPSC-Mg). Signaling assay in wild type (WT) and TREM2-KO iPSC-Mg. (a) Briefly, 15,000 cell/well of commercially available IPSC derived microglial cells (cellular dynamics) were thawed according to manufacturer's instruction and plated 24 h in maintenance medium in PEI coated plates. IPSC-mg were treated during indicated times with vehicle, activating TREM2 antibody (10 μg/ml) or liposomal particles (250 μ/ml). phosphorylated-spleen tyrosine kinase (p-Syk) signal was measured using AlphaLISA assay. Each data point represents a single well ($n = 4$ per conditions) and bar and whiskers represent mean $\pm$ *SEM* and data were reproduced across two independent experiments. (b) ATP content in AF1828 or liposome stimulated iPSC-Mg. In parallel to the experiment described in (a), cells were treated with liposome during 6 h (left) and 24 h (right) and cell ATP content measured using cell titer glow assay (Promega, four wells per condition). (c) independently derived iPSC-Mg were seeded and differentiated in 384-well plate. After maturation, cells were treated with anti-TREM2 antibody (5 min), dioleoyl-phosphocholine (DOPS) or palmitoyl-phosphocholine (DPPC) liposomes (2 min). p-Syk as well as total Syk levels were quantified by AlphaLISA assays and ratio reported (each individual marker reported in Supplementary Figure S4B). Data are representative of three independent experiments

first incubation step, substrates for phagocytosis, namely pHrodo-*E. coli* particles (Figure 5a–c) or fluorescent Aβ42 particles (Figure 6a,c), were added to the cells and THP1 fluorescence acquisition overtime was assessed by Incucyte S3 live imaging, as previously described (McQuade et al., 2020). The TREM2 targeting antibody increased *E. coli* phagocytosis capacity in WT THP1, and this function was Syk dependent, as R406 treatment abrogated the antibody stimulation effect (Figure 5a,c). Of note, R406 alone did not alter the basal

phagocytosis activity of WT THP1 cells treated with medium only (Figure 5a,c). Similarly, DOPEG, DOPS and DOPEth liposomes increased phagocytosis capacities in WT THP1 cells, in a Syk-dependent manner (Figure 5b,c). DPPC did not significantly enhance *E.coli* particle phagocytosis compared to medium condition (Figure 5b,c). Of note, none of the agonist antibody or liposomes significantly changed the phagocytosis capacities of TREM2-KO THP1 cells (Figure 5b lower panels, quantified in Figure 5c). Similar results were

obtained with phagocytosis of fluorescent Aβ42 although TREM2 agonists increased phagocytosis of Aβ42 more modestly than *E.coli* phagocytosis (Figure 6a,c). In TREM2-KO THP1 cells, as previously observed with *E.coli* particles, none of the applied treatments (antibody or liposome) modified Aβ phagocytosis. These results demonstrate that, similarly to an agonist TREM2 antibody, the liposomes were able to enhance TREM2 mediated cellular function for over 10 hours.

3.6 | Liposomal particles are active on human IPSC-derived microglia

With an activity validated in native TREM2 expressing THP1 cells, we next questioned if the newly established liposomal TREM2 agonists could be active on human microglial cells. We first used TREM2 WT (or common variant) and KO iPSC derived microglial cells (iPSC-Mg) commercially available from Cellular Dynamics. In TREM2 WT cells, stimulation with DOPEG or DOPS, but not DPPC liposomes led to a very fast increase in p-Syk levels at 2 min already, returning close to baseline at 5 min, while the p-Syk signal induced by the TREM2 agonist antibody declined only at 10 min time point (Figure 7a). Activation kinetics were therefore even faster than in THP1 cells. The magnitude of response to both agonist types were similar. As expected, no p-Syk signal was elicited in TREM2-KO cells, which further underlines the specificity of these agonists.

TREM2 stimulation had been previously shown to boost cell energy metabolism. Accordingly, both TREM2 antibody and DOPEG liposomes increased ATP levels in iPSC-Mg at 6 h, while both were inactive in the TREM2-KO line (Figure 7b, left panel). DPPC liposomes were inactive. Of note, as previously described, TREM2-KO cells were anergic, that is, with low ATP levels. At longer time points, only TREM2 antibody stimulation led to a sustained increase in ATP levels (Figure 7b, right panel). To expand these first data, liposomes were shipped at 4°C to two different laboratories from a large European IMI-funded consortium Phago (studying TREM2 and CD33) and were tested on lab-generated human iPSC-Mg from iPSC lines BIONi010-C (isogenic control line) and BIONi010-C-17 (TREM2 KO) in 96-well format (Supplemental Figure S4A) and 384-well format (Figure 7c). DOPEG and DOPS liposomes dose-dependently increased the p-Syk signal (maximum from the earliest time point at 2 min) with no effect in TREM2-KO cells. TREM2 antibody AF1828 response was again slightly delayed with a peak at 5 min (data not shown) and a larger amplitude than with liposomes (Supplemental Figure S4A). Of note, the TREM2-KO had a much lower basal p-Syk/total Syk ratio. Loss of TREM2 protein, both soluble and total cellular, was confirmed in these TREM2-KO iPSC-Mg (Supplementary Figure S4C, left panel). A more thorough concentration-response analysis was conducted using an optimized 384-well plate format developed for high throughput screening. Activity was measured at 2 min for liposomes and at 5 min for antibody corresponding to the technical maximal response for each of the agonists. In the control iPSC-microglia, DOPS liposomes increased the p-Syk signal with an EC_{50} value of 3.4 μg/ml, while

DPPC liposomes were inactive (Figure 7c). TREM2 antibody AF1828 response had again a higher magnitude, in the order of 6-fold compared to 2-fold for DOPS liposomes. Both agonists were inactive in TREM2-KO cells. At this point, it is not understood why the antibody response is stronger than for DOPS liposomes in the BIONi010C IPS line but are similar in the Cellular Dynamics IPS. Possibly, the very fast kinetic of the liposome response might make it difficult to capture the optimal short time point, especially in high throughput screening conditions. As a control using stimulation with concanavalin A, we demonstrated that the phosphorylation of Syk was not broadly compromised in TREM2-KO cells (supplemental Figure S4C right).

4 | DISCUSSION

We report the optimization of liposomes as specific agonists of the TREM2 receptor versus the closely related TREM1 receptor, validated both in TREM2 overexpressing cell lines and in native cellular systems. The optimal lipid composition of 50% PL (18% active PL and 32% buffer phosphatidylcholine), and 50% CHO, analogous to biological membranes, provides homogeneously sized liposome preparations with strong stability over several months when stored at 4°C. This formulation is critical to observe large differential between the agonist activity of PS and inactivity of the neutral phosphatidylcholine equivalent, which consequently can be used as relevant liposome negative control. Higher phosphatidylcholine concentrations lead to unexpected activity and cannot be used as a negative control. TREM2 activation was initially measured at an early event of the signal transduction by assessing phosphorylated Syk levels and confirmed with downstream markers and cellular integrated responses. Syk phosphorylation was notably faster with active liposomes (maximal response reached at 2 min) as compared to TREM2 agonist antibodies, possibly suggesting a faster/more efficient crosslinking of TREM2 molecules by the multivalent liposomes than by divalent antibodies.

This stable formulation enabled to conduct analysis of the structure activity relationship of PL heads as TREM2 agonist. Phosphoglycerolipids with a net negative charge activate TREM2 while neutral PL are inactive. A similar trend is shown with sphingolipids, especially with the highly charged sulfo-galactoceramide compared to the unsulfated form, indicating that phosphatidyl can be replaced by other negative charges. The robustness of the results is supported by similar findings in two TREM2wt/DAP12 cell lines with different expression levels as well as in a TREM2-R47H cell line. The key findings were further confirmed in THP1 cells and iPSC-derived microglia both natively expressing TREM2. The TREM2 agonist activity correlates with the liposome particle overall charge (zeta potential) rather than the absolute charge of the PL head. The zeta potential could influence the accessibility of liposomes onto TREM2 molecules expressed on cell surface and/or could modulate the interaction between the two partners. The minimal head phosphatidic acid has a good agonist activity and addition of short alkyl chain (even one carbon with methanol) can further increase activity, suggesting an optimized warhead for TREM2 agonism, although again such small modifications also decreased the

particle zeta potential in parallel. A significant limitation for such liposomes is that serum concentrations as low as 0.5% strongly affected the liposome activity possibly due to formation of a corona of serum cationic proteins (Montizaan et al., 2020) and will have to be overcome for in vivo use. Potential modifications of the outer shell of liposomes such as with polyethylene glycol have been shown to improve liposome bioavailability (Ogier et al., 2009) but could also interfere with the docking on TREM2 by steric hindrance. Overall, the mapping of the minimal TREM2 warhead could be used to design synthetic molecules containing multiple copies, as for example on dendrimers, of the minimal warhead to mimic the liposome multivalent configuration (Lo et al., 2013).

This detailed SAR study highlights some important differences with previous literature reports on activation of TREM2 by PLs. Using lipids coated plates, Sudom and colleagues reported strong TREM2 binding to the neutral phosphoethanolamine versus phosphatidic acid in line with previous claims (Cannon et al., 2012; Kober et al., 2016; Sudom et al., 2018), while the exact opposite is demonstrated when measuring agonist activity with the present liposome formulation. Similarly, cells exposed to lipid coated plates overnight express strong response to phosphatidylcholine, SM, and phosphatidylethanolamine using a TREM2 reporter assay (Wang et al., 2015; Poliani et al., 2015; Shirotani et al., 2019), while all three PLs were TREM2 inactive when exposed on liposomes. Of note, we used highly pure neutral SM-choline while brain purified SM is more heterogeneous and can contain charged SM. Using liposome with different formulation (30%/70% PL/phosphatidylcholine, no CHO), Nugent reported that phosphatidylcholine and SM activated TREM2 as efficiently as phosphatidylserine in TREM2 overexpressing cells (Nugent et al., 2020). Indeed, we could confirm Nugent's findings when using formulation 1 (Figure 1), in sharp contrast to our results with the optimized formulation 3 liposome composition where both are inactive. Therefore, physiological liposome composition does lead to a significantly different structure activity relationship of TREM2 activation by PLs. Another caveat of liposomes is the possible oxidation of lipids upon storage, which can also lead to TREM2 agonist activity (as shown with oxPAPC) confirming recently published data (Dong et al., 2021). Interestingly, the optimized liposomes displayed similar activity (EC_{50}) in HEK cells expressing TREM2 WT and R47H variants. Our results are again at odd with the much lower affinity of TREM2 R47H versus WT ECD reported for plate coated-phosphatidylserine (Sudom et al., 2018), which has been widely used as proof of a TREM2 R47H loss-of-function for PL binding. The same authors also reported that pure DOPS liposomes were less effective in activating TREM2 R47H in a similar TREM2/DAP12 recombinant cell line, but the low potency of their liposome preparations was leading to only partial activation levels precluding EC_{50} determinations. In addition, there was no control of the respective level of TREM2 and DAP12 expression in the cell lines they used, while we noted here that differences in DAP12 expression levels can significantly affect magnitude of p-Syk activation. Comparison in cellular systems with native and comparable expression levels of TREM2 WT, R47H, and DAP12 would be very important, but our present results would argue that the TREM2 R47H mutation does not appear to impair TREM2 activation by phosphatidylserine in a more controlled and physiological liposome configuration.

Currently, our optimized TREM2 liposomes have some limitations since DOPS liposomes, unlike DPPC, can fuse with live cell membranes after 30 min and are sensitive to traces (0.5%) of serum protein (discussed above). The membrane fusion could be responsible for the non- TREM2, non-Syk dependent AKT activation response observed in THP1 cells. In this context, the use of Syk inhibitor R406 is important to delineate the TREM2-dependent component of the phenotype when TREM2 gene deletion is not available.

The strong TREM2 agonist activity of liposomes led to significant increase in THP1 phagocytosis activity both using *E. coli* and Aβ42 as substrates. While Aβ42 has been presented as a TREM2 binder, the effect on *E. coli* phagocytosis underlies an overall increase in THP1 phagocytosis activity that was enhanced for many hours (over 10 h) far outlasting the transient p-Syk observed, suggestive of a durable change in a THP1 integrated biological response and cell metabolism. Liposomes led to a greater phagocytosis enhancement than the extensively used TREM2 antibody AF1828. In human iPS-derived microglia, liposomes were activators of the TREM2 signaling with a similar active lipid selectivity and led to a increase in cellular metabolism (ATP), a known TREM2-dependent cellular parameter as further indicated by the observed anergy of TREM2-KO cells. At this point, it is not understood why the TREM2 antibody p-Syk response is stronger than for DOPS liposomes in the BIONi010C IPS line but are similar in the Cellular Dynamics IPS. The very fast kinetic of the p-Syk response for liposomes (already declining after 2 min) might lead to underestimation of the peak response especially in multiwell screening conditions used for the BIONi010C line where such short timings are difficult to standardize.

Attempting to mimic endogenous TREM2 ligands, the present liposomes represent robust and highly selective TREM2 agonist tools most likely acting on the TREM2 IgV fold, complementing the widely used TREM2 agonist antibodies targeting TREM2 stalk domain. They enabled to revisit the detailed structure activity relationship of phosphoglycolipid polar heads as TREM2 agonists using a more biologically relevant exposure of lipids heads exposed on liposomes. We characterized the shortest maximally active sidechain for optimized TREM2 agonist activity that can be used by simple addition to cellular cultures. Interestingly, PS liposomes have very similar activity on both TREM2 common variant and TREM2 R47H mutant. Activity was further confirmed in two different TREM2 natively expressing systems. While likely not usable in vivo, such tools should be useful in further studies of TREM2 biology in cellular systems and the polar head structural information could be used in the design of synthetic chemical TREM2 agonists.

AUTHOR CONTRIBUTIONS

DATA AVAILABILITY STATEMENT
Data will be made available upon reasonable request to corresponding authors as well as detailed protocole for liposome preparation

ORCID
Jennifer M. Pocock https://orcid.org/0000-0001-5812-9331
Laurent Pradier https://orcid.org/0000-0001-6022-0951

REFERENCES
Andreone, B. J., Przybyla, L., Llapashtica, C., Rana, A., Davis, S. S., van Lengerich, B., Lin, K., Shi, J., Mei, Y., Astarita, G., Di Paolo, G., Sandmann, T., Monroe, K. M., & Lewcock, J. W. (2020). Alzheimer's-associated PLCgamma2 is a signaling node required for both TREM2 function and the inflammatory response in human microglia. *Nat Neurosci*, 23(8), 927–938.
Atagi, Y., Liu, C. C., Painter, M. M., Chen, X. F., Verbeeck, C., Zheng, H., Li, X., Rademakers, R., Kang, S. S., Xu, H., Younkin, S., Das, P., Fryer, J. D., & Bu, G. (2015). Apolipoprotein E Is a Ligand for Triggering Receptor Expressed on Myeloid Cells 2 (TREM2). *J Biol Chem*, 290(43), 26043–26050.
Borroni, B., Ferrari, F., Galimberti, D., Nacmias, B., Barone, C., Bagnoli, S., Fenoglio, C., Piaceri, I., Archetti, S., Bonvicini, C., Gennarelli, M., Turla, M., Scarpini, E., Sorbi, S., & Padovani, A. (2014). Heterozygous TREM2 mutations in frontotemporal dementia. *Neurobiol Aging*, 35(4), 934 e937-910.
Cannon, J. P., O'Driscoll, M., & Litman, G. W. (2012). Specific lipid recognition is a general feature of CD300 and TREM molecules. *Immunogenetics*, 64(1), 39–47.
Cosker, K., Mallach, A., Limaye, J., Piers, T. M., Staddon, J., Neame, S. J., Hardy, J., & Pocock, J. M. (2021). Microglial signalling pathway deficits associated with the patient derived R47H TREM2 variants linked to AD indicate inability to activate inflammasome. *Sci Rep*, 11(1), 13316.
Cuyvers, E., Bettens, K., Philtjens, S., Van Langenhove, T., Gijselinck, I., van der Zee, J., Engelborghs, S., Vandenbulcke, M., Van Dongen, J., Geerts, N., Maes, G., Mattheijssens, M., Peeters, K., Cras, P., Vandenberghe, R., De Deyn, P. P., Van Broeckhoven, C., Cruts, M., Sleegers, K. & BELNEU consortium. (2014). Investigating the role of rare heterozygous TREM2 variants in Alzheimer's disease and frontotemporal dementia. *Neurobiol Aging*, 35(3), 726.e711–729.
Dong, Y., D'Mello, C., Pinsky, W., Lozinski, B. M., Kaushik, D. K., Ghorbani, S., Moezzi, D., Brown, D., Melo, F. C., Zandee, S., Vo, T., Prat, A., Whitehead, S. N., & Yong, V. W. (2021). Oxidized phosphatidylcholines found in multiple sclerosis lesions mediate neurodegeneration and are neutralized by microglia. *Nat Neurosci*, 24(4), 489–503.
Ellwanger, D. C., Wang, S., Brioschi, S., Shao, Z., Green, L., Case, R., Yoo, D., Weishuhn, D., Rathanaswami, P., Bradley, J., Rao, S., Cha, D., Luan, P., Sambashivan, S., Gilfillan, S., Hasson, S. A., Foltz, I. N., Van Lookeren Campagne, M. & Colonna, M. (2021). Prior activation state shapes the microglia response to antihuman TREM2 in a mouse model of Alzheimer's disease. *Proc Natl Acad Sci U S A*, 118(3), e2017742118.
Ewers, M., Franzmeier, N., Suarez-Calvet, M., Morenas-Rodriguez, E., Caballero, M. A. A., Kleinberger, G., Piccio, L., Cruchaga, C., Deming, Y., Dichgans, M., Trojanowski, J. Q., Shaw, L. M., Weiner, M. W., Haass, C. & Alzheimer's Disease Neuroimaging, I. (2019). Increased soluble TREM2 in cerebrospinal fluid is associated with reduced cognitive and clinical decline in Alzheimer's disease. *Sci Transl Med*, 11(507), eaav6221.
Fassler, M., Rappaport, M. S., Cuno, C. B., & George, J. (2021). Engagement of TREM2 by a novel monoclonal antibody induces activation of microglia and improves cognitive function in Alzheimer's disease models. *J Neuroinflammation*, 18(1), 19.
Garcia-Reitboeck, P., Phillips, A., Piers, T. M., Villegas-Llerena, C., Butler, M., Mallach, A., Rodrigues, C., Arber, C. E., Heslegrave, A., Zetterberg, H., Neumann, H., Neame, S., Houlden, H., Hardy, J., & Pocock, J. M. (2018). Human induced pluripotent stem cell-derived microglia-like cells harboring TREM2 missense mutations show specific deficits in phagocytosis. *Cell Rep*, 24(9), 2300–2311.
Griciuc, A., Patel, S., Federico, A. N., Choi, S. H., Innes, B. J., Oram, M. K., Cereghetti, G., McGinty, D., Anselmo, A., Sadreyev, R. I., Hickman, S. E., El Khoury, J., Colonna, M., & Tanzi, R. E. (2019). TREM2 Acts Downstream of CD33 in Modulating Microglial Pathology in Alzheimer's Disease. *Neuron*, 103(5), 820–835.e827.
Guerreiro, R., Bilgic, B., Guven, G., Bras, J., Rohrer, J., Lohmann, E., Hanagasi, H., Gurvit, H., & Emre, M. (2013). Novel compound heterozygous mutation in TREM2 found in a Turkish frontotemporal dementia-like family. *Neurobiol Aging*, 34(12), 2890.e2891–2895.
Haenseler, W., Sansom, S. N., Buchrieser, J., Newey, S. E., Moore, C. S., Nicholls, F. J., Chintawar, S., Schnell, C., Antel, J. P., Allen, N. D., Cader, M. Z., Wade-Martins, R., James, W. S., & Cowley, S. A. (2017). A highly efficient human pluripotent stem cell microglia model displays a neuronal-co-culture-specific expression profile and inflammatory response. *Stem Cell Reports*, 8(6), 1727–1742.
Ibach, M., Mathews, M., Linnartz-Gerlach, B., Theil, S., Kumar, S., Feederle, R., Brustle, O., Neumann, H., & Walter, J. (2021). A reporter cell system for the triggering receptor expressed on myeloid cells 2 reveals differential effects of disease-associated variants on receptor signaling and activation by antibodies against the stalk region. *Glia*, 69(5), 1126–1139.
Ingolfsson, H. I., Melo, M. N., van Eerden, F. J., Arnarez, C., Lopez, C. A., Wassenaar, T. A., Periole, X., de Vries, A. H., Tieleman, D. P., & Marrink, S. J. (2014). Lipid organization of the plasma membrane. *J Am Chem Soc*, 136(41), 14554–14559.
Joshi, P., Riffel, F., Satoh, K., Enomoto, M., Qamar, S., Scheiblich, H., Villacampa, N., Kumar, S., Theil, S., Parhizkar, S., Haass, C., Heneka, M. T., Fraser, P. E., St George-Hyslop, P., & Walter, J. (2021). Differential interaction with TREM2 modulates microglial uptake of modified Abeta species. *Glia*, 69(12), 2917–2932.

Keren-Shaul, H., Spinrad, A., Weiner, A., Matcovitch-Natan, O., Dvir-Szternfeld, R., Ulland, T. K., David, E., Baruch, K., Lara-Astaiso, D., Toth, B., Itzkovitz, S., Colonna, M., Schwartz, M., & Amit, I. (2017). A unique microglia type associated with restricting development of Alzheimer's disease. *Cell*, 169(7), 1276–1290.e1217.

Kim, S. M., Mun, B. R., Lee, S. J., Joh, Y., Lee, H. Y., Ji, K. Y., Choi, H. R., Lee, E. H., Kim, E. M., Jang, J. H., Song, H. W., Mook-Jung, I., Choi, W. S., & Kang, H. S. (2017). TREM2 promotes Abeta phagocytosis by upregulating C/EBPalpha-dependent CD36 expression in microglia. *Sci Rep*, 7(1), 11118.

Kober, D. L., Alexander-Brett, J. M., Karch, C. M., Cruchaga, C., Colonna, M., Holtzman, M. J., & Brett, T. J. (2016). Neurodegenerative disease mutations in TREM2 reveal a functional surface and distinct loss-of-function mechanisms. *Elife*, 5(e20391), 1–24.

Krasemann, S., Madore, C., Cialic, R., Baufeld, C., Calcagno, N., El Fatimy, R., Beckers, L., O'Loughlin, E., Xu, Y., Fanek, Z., Greco, D. J., Smith, S. T., Tweet, G., Humulock, Z., Zrzavy, T., Conde-Sanroman, P., Gacias, M., Weng, Z., Chen, H., … Butovsky, O. (2017). The TREM2-APOE pathway drives the transcriptional phenotype of dysfunctional microglia in neurodegenerative diseases. *Immunity*, 47(3), 566–581.e569.

Lee, C. Y. D., Daggett, A., Gu, X., Jiang, L. L., Langfelder, P., Li, X., Wang, N., Zhao, Y., Park, C. S., Cooper, Y., Ferando, I., Mody, I., Coppola, G., Xu, H., & Yang, X. W. (2018). Elevated TREM2 gene dosage reprograms microglia responsivity and ameliorates pathological phenotypes in Alzheimer's disease models. *Neuron*, 97(5), 1032–1048.e1035.

Li, X., Sun, Y., Gong, L., Zheng, L., Chen, K., Zhou, Y., Gu, Y., Xu, Y., Guo, Q., Hong, Z., Ding, D., Fu, J., & Zhao, Q. (2020). A novel homozygous mutation in TREM2 found in a Chinese early-onset dementia family with mild bone involvement. *Neurobiol Aging*, 86, 201.e201–201.e207.

Lo, S. T., Kumar, A., Hsieh, J. T., & Sun, X. (2013). Dendrimer nanoscaffolds for potential theranostics of prostate cancer with a focus on radiochemistry. *Mol Pharm*, 10(3), 793–812.

McQuade, A., Kang, Y. J., Hasselmann, J., Jairaman, A., Sotelo, A., Coburn, M., Shabestari, S. K., Chadarevian, J. P., Fote, G., Tu, C. H., Danhash, E., Silva, J., Martinez, E., Cotman, C., Prieto, G. A., Thompson, L. M., Steffan, J. S., Smith, I., Davtyan, H., … Blurton-Jones, M. (2020). Gene expression and functional deficits underlie TREM2-knockout microglia responses in human models of Alzheimer's disease. *Nat Commun*, 11(1), 5370.

Montizaan, D., Yang, K., Reker-Smit, C., & Salvati, A. (2020). Comparison of the uptake mechanisms of zwitterionic and negatively charged liposomes by HeLa cells. *Nanomedicine*, 30, 102300.

Nugent, A. A., Lin, K., van Lengerich, B., Lianoglou, S., Przybyla, L., Davis, S. S., Llapashtica, C., Wang, J., Kim, D. J., Xia, D., Lucas, A., Baskaran, S., Haddick, P. C. G., Lenser, M., Earr, T. K., Shi, J., Dugas, J. C., Andreone, B. J., Logan, T., … Di Paolo, G. (2020). TREM2 regulates microglial cholesterol metabolism upon chronic phagocytic challenge. *Neuron*, 105(5), 837–854.e839.

Ogier, J., Arnauld, T., & Doris, E. (2009). Recent advances in the field of nanometric drug carriers. *Future Med Chem*, 1(4), 693–711.

Paloneva, J., Manninen, T., Christman, G., Hovanes, K., Mandelin, J., Adolfsson, R., Bianchin, M., Bird, T., Miranda, R., Salmaggi, A., Tranebjaerg, L., Konttinen, Y., & Peltonen, L. (2002). Mutations in two genes encoding different subunits of a receptor signaling complex result in an identical disease phenotype. *Am J Hum Genet*, 71(3), 656–662.

Parhizkar, S., Arzberger, T., Brendel, M., Kleinberger, G., Deussing, M., Focke, C., Nuscher, B., Xiong, M., Ghasemigharagoz, A., Katzmarski, N., Krasemann, S., Lichtenthaler, S. F., Muller, S. A., Colombo, A., Monasor, L. S., Tahirovic, S., Herms, J., Willem, M., Pettkus, N., … Haass, C. (2019). Loss of TREM2 function increases amyloid seeding but reduces plaque-associated ApoE. *Nat Neurosci*, 22(2), 191–204.

Piers, T. M., Cosker, K., Mallach, A., Johnson, G. T., Guerreiro, R., Hardy, J., & Pocock, J. M. (2020). A locked immunometabolic switch underlies TREM2 R47H loss of function in human iPSC-derived microglia. *FASEB J*, 34(2), 2436–2450.

Poliani, P. L., Wang, Y., Fontana, E., Robinette, M. L., Yamanishi, Y., Gilfillan, S., & Colonna, M. (2015). TREM2 sustains microglial expansion during aging and response to demyelination. *J Clin Invest*, 125(5), 2161–2170.

Schlepckow, K., Monroe, K. M., Kleinberger, G., Cantuti-Castelvetri, L., Parhizkar, S., Xia, D., Willem, M., Werner, G., Pettkus, N., Brunner, B., Sulzen, A., Nuscher, B., Hampel, H., Xiang, X., Feederle, R., Tahirovic, S., Park, J. I., Prorok, R., Mahon, C., … Haass, C. (2020). Enhancing protective microglial activities with a dual function TREM2 antibody to the stalk region. *EMBO Mol Med*, 12(4), e11227.

Scott-Hewitt, N., Perrucci, F., Morini, R., Erreni, M., Mahoney, M., Witkowska, A., Carey, A., Faggiani, E., Schuetz, L. T., Mason, S., Tamborini, M., Bizzotto, M., Passoni, L., Filipello, F., Jahn, R., Stevens, B., & Matteoli, M. (2020). Local externalization of phosphatidylserine mediates developmental synaptic pruning by microglia. *EMBO J*, 39(16), e105380.

Shirotani, K., Hori, Y., Yoshizaki, R., Higuchi, E., Colonna, M., Saito, T., Hashimoto, S., Saito, T., Saido, T. C., & Iwata, N. (2019). Aminophospholipids are signal-transducing TREM2 ligands on apoptotic cells. *Sci Rep*, 9(1), 7508.

Song, W. M., Joshita, S., Zhou, Y., Ulland, T. K., Gilfillan, S., & Colonna, M. (2018). Humanized TREM2 mice reveal microglia-intrinsic and -extrinsic effects of R47H polymorphism. *J Exp Med*, 215(3), 745–760.

Sudom, A., Talreja, S., Danao, J., Bragg, E., Kegel, R., Min, X., Richardson, J., Zhang, Z., Sharkov, N., Marcora, E., Thibault, S., Bradley, J., Wood, S., Lim, A. C., Chen, H., Wang, S., Foltz, I. N., Sambashivan, S., & Wang, Z. (2018). Molecular basis for the loss-of-function effects of the Alzheimer's disease-associated R47H variant of the immune receptor TREM2. *J Biol Chem*, 293(32), 12634–12646.

Takahashi, K., Rochford, C. D., & Neumann, H. (2005). Clearance of apoptotic neurons without inflammation by microglial triggering receptor expressed on myeloid cells-2. *J Exp Med*, 201(4), 647–657.

Ulland, T. K., Song, W. M., Huang, S. C., Ulrich, J. D., Sergushichev, A., Beatty, W. L., Loboda, A. A., Zhou, Y., Cairns, N. J., Kambal, A., Loginicheva, E., Gilfillan, S., Cella, M., Virgin, H. W., Unanue, E. R., Wang, Y., Artyomov, M. N., Holtzman, D. M., & Colonna, M. (2017). TREM2 maintains microglial metabolic fitness in Alzheimer's disease. *Cell*, 170(4), 649–663 e613.

Vilalta, A., Zhou, Y., Sevalle, J., Griffin, J. K., Satoh, K., Allendorf, D. H., De, S., Puigdellivol, M., Bruzas, A., Burguillos, M. A., Dodd, R. B., Chen, F., Zhang, Y., Flagmeier, P., Needham, L. M., Enomoto, M., Qamar, S., Henderson, J., Walter, J., … Brown, G. C. (2021). Wild-type sTREM2 blocks Abeta aggregation and neurotoxicity, but the Alzheimer's R47H mutant increases Abeta aggregation. *J Biol Chem*, 296, 100631.

Wang, S., Mustafa, M., Yuede, C. M., Salazar, S. V., Kong, P., Long, H., Ward, M., Siddiqui, O., Paul, R., Gilfillan, S., Ibrahim, A., Rhinn, H., Tassi, I., Rosenthal, A., Schwabe, T. & Colonna, M. (2020). Anti-human TREM2 induces microglia proliferation and reduces pathology in an Alzheimer's disease model. *J Exp Med*, 217(9), e20200785.

Wang, Y., Cella, M., Mallinson, K., Ulrich, J. D., Young, K. L., Robinette, M. L., Gilfillan, S., Krishnan, G. M., Sudhakar, S., Zinselmeyer, B. H., Holtzman, D. M., Cirrito, J. R., & Colonna, M. (2015). TREM2 lipid sensing sustains the microglial response in an Alzheimer's disease model. *Cell*, 160(6), 1061–1071.

Yeh, F. L., Wang, Y., Tom, I., Gonzalez, L. C., & Sheng, M. (2016). TREM2 binds to apolipoproteins, including APOE and CLU/APOJ, and thereby facilitates uptake of amyloid-beta by microglia. *Neuron*, *91*(2), 328–340.

Zhao, Y., Wu, X., Li, X., Jiang, L. L., Gui, X., Liu, Y., Sun, Y., Zhu, B., Pina-Crespo, J. C., Zhang, M., Zhang, N., Chen, X., Bu, G., An, Z., Huang, T. Y., & Xu, H. (2018). TREM2 is a receptor for beta-amyloid that mediates microglial function. *Neuron*, *97*(5), 1023–1031. e1027.

Zhou, Y., Song, W. M., Andhey, P. S., Swain, A., Levy, T., Miller, K. R., Poliani, P. L., Cominelli, M., Grover, S., Gilfillan, S., Cella, M., Ulland, T. K., Zaitsev, K., Miyashita, A., Ikeuchi, T., Sainouchi, M., Kakita, A., Bennett, D. A., Schneider, J. A., ... Colonna, M. (2020). Human and mouse single-nucleus transcriptomics reveal TREM2-dependent and TREM2-independent cellular responses in Alzheimer's disease. *Nat Med*, *26*(1), 131–142.

SUPPORTING INFORMATION

Additional supporting information can be found online in the Supporting Information section at the end of this article.